Phytoplankton Kinetics in the Chesapeake Bay Eutrophication Model

Carl F. Cerco

Introduction

Modern eutrophication modeling of Chesapeake Bay commenced in 1987. In that year, an effort was completed that applied three-dimensional hydrodynamic and eutrophication models to data collected in 1965, 1984, and 1985 (HydroQual 1987). Summer-average, steady-state conditions were modeled independently in each year. The model provided credible representations of historic and contemporary conditions in the Bay and tributaries. Despite the success of the modeling effort, limitations were apparent. The chief limitation was absence of a predictive model of sediment-water interactions. A second limitation was the steady-state nature of the analysis. The steady-state model allowed no influence of conditions in previous years or seasons on summer-average water quality.

A succeeding model effort combined an intertidal, three-dimensional hydrodynamic model (Johnson et al. 1993), a three-dimensional eutrophication model (Cerco and Cole 1993), and a predictive sediment diagenesis model (DiToro and Fitzpatrick 1993). The model package was applied in one continuous simulation to the period 1984-1986 and proved successful in simulating transport, eutrophication processes, and sediment-water interactions. Subsequently, the model package was employed in management scenarios (Cerco 1995a) and in analysis of long-term trends in eutrophication (Cerco 1995b).

Most recently, refinements were added to the 1993 model package including increased grid resolution within the major western-shore tributaries, extension of the grid beyond the mouth of the bay onto the continental shelf, direct simulation of living resources (zooplankton, submerged aquatic vegetation, and benthos), and extension of the validation period to include contemporary data (Cerco and Meyers 2000). The refinements also encompassed revisions to the eutrophication kinetics. The refined phytoplankton kinetics are the subject of the present paper.

Chesapeake Bay

Physical Description

The Chesapeake Bay system (Figure 1) consists of the mainstem bay, five major western-shore tributaries, and a host of lesser tributaries and embayments. The mainstem is roughly 300 km long, 8 to 48 km wide, and 8 m average depth. A deep trench with depths to 50 m runs up the center of the mainstem.

Total drainage area of the Bay is 166,000 km^2. The primary source of freshwater to the system is the Susquehanna River (. 64% of total gauged freshwater flow) which empties into the northernmost extent of the Bay. Other major freshwater sources are the Potomac (. 19%) and James Rivers (. 12%). The remaining western-shore tributaries, the York (. 3%), the Rappahannock (. 3%), and the Patuxent (< 1%) contribute only small fractions of the total

freshwater flow to the Bay.

The mainstem bay and major tributaries are classic examples of partially-mixed estuaries (Pritchard 1967). When flows in these estuaries are averaged over lengthy time periods, generally more than fifteen days, a net longitudinal circulation is evident. Longitudinal density gradients push bottom water upstream and enhance flow of surface water downstream. The volume of the density-induced flow vastly exceeds the volume of freshwater runoff.

Bottom-Water Hypoxia

During the summer months, bottom waters of the mainstem bay are characterized by hypoxic (low dissolved oxygen) or anoxic (no dissolved oxygen) conditions. Longitudinal and lateral extent of hypoxia are determined by the geometry of the trench that runs up the center of the Bay. On occasion, hypoxic water extends from the bottom to within a few meters of the surface but summer-average oxygen concentration within the surface mixed layer is usually 6 g m^{-3} or greater.

Bottom-water hypoxia occurs at recurrent, predictable time intervals. The onset is in late May when spring warming enhances respiration in benthic sediments. Decay of material deposited in spring and in previous years removes oxygen from bottom water. Density stratification prevents mixing of oxygenated surface water downwards. Low-oxygen conditions continue through the summer, maintained by respiration in bottom water. In mid-September, autumn winds end the hypoxic period by mixing surface water down to the bottom. Respiration in bottom water, diminished by cool temperature, is insufficient to re-establish hypoxia following the mixing event.

Spring Phytoplankton Bloom

A second recurring phenomenon in the Bay is the spring phytoplankton bloom. The spring bloom consists primarily of diatoms including *Skeletonema*, *Leptocylindrus*, and *Cyclotella* (Marshall and Lacouture 1986). The bloom usually commences in February and ends precipitously in late May. The bloom is characterized by high chlorophyll concentrations throughout the water column. At times, a subsurface chlorophyll maximum occurs. During summer, chlorophyll concentrations and algal biomass are generally less than in spring and restricted to surface waters. Despite the disparity in biomass, primary production in summer exceeds production in spring (Malone et al. 1988).

Although the bloom occurs regularly, the magnitude and spatial extent of the bloom vary from year to year. Factors affecting this variability are not well known. The occurrence and apparent survival of viable algae at great depth, in the absence of light, also remain unexplained.

The occurrence and magnitude of the spring bloom are linked to subsequent bottom-water anoxia. A spring peak in carbon deposition to sediment results from the algal bloom (Boynton and Kemp 1985) and the decay of this fresh organic matter contributes to oxygen demand. A subtle, and potentially more important link, is through a nutrient trapping mechanism (Malone et al. 1988). Algae during the bloom take up nutrients in spring runoff. Predation and algal mortality result in the transfer of nutrients, in particulate organic form, to benthic sediments. In summer, the

nutrients are mineralized in the sediments and released to the water column. Nutrients released from the sediment support summer algal production. Carbon produced by algae settles to bottom waters, decays, and consumes oxygen. Diminished oxygen in bottom water enhances sediment nutrient release, especially of ammonium. The nutrient release continues the cycle of benthic release, algal production, and oxygen consumption.

The Chesapeake Bay Estuary Model Package

The Conservation of Mass Equation

The hydrodynamic and eutrophication models operate by dividing the spatial continuum of the bay into a grid of discrete cells (Figure 2). The grid for the present study contained 2100 cells (roughly 1.5 x 3 km) in the surface plane and one to nineteen cells (1.5 to 2 m thick) in the vertical. Total number of cells in the grid was 10196. CE-QUAL-ICM treats each cell as a control volume, which exchanges material with its adjacent cells. CE-QUAL-ICM solves, for each volume and for each state variable, the three-dimensional conservation of mass equation:

$$\frac{d\,V_i\,C_i}{d\,t} = \sum_{j=1}^{n} Q_j\;\; C_j^{*} + \sum_{j=1}^{n} A_j\;\; D_j\;\; \frac{d\,C}{d\,x_j} + \sum S_i \qquad (1)$$

V_i = volume of ith control volume (m^3)
C_i = concentration in ith control volume (g m^{-3})
Q_j = volumetric flow across flow face j of ith control volume (m^3 sec^{-1})
C^*_j = concentration in flow across flow face j (g m^{-3})
A_j = area of flow face j (m^2)
D_j = diffusion coefficient at flow face j (m^2 sec^{-1})
n = number of flow faces attached to ith control volume
S_i = external loads and kinetic sources and sinks in ith control volume (g sec^{-1})
t, x = temporal and spatial coordinates

Solution to the mass-conservation equation is via the finite-difference method using the QUICKEST algorithm (Leonard 1979) in the horizontal directions and a Crank-Nicolson scheme in the vertical direction.

The Eutrophication Model

The central issues in the water quality model are computation of algal biomass and dissolved oxygen. Through primary production of carbon, algae provide the energy required by the ecosystem to function. Excessive primary production is detrimental, however, since its decomposition, in the water and sediments, consumes oxygen. Dissolved oxygen is necessary to support the life functions of higher organisms and is considered an indicator of the 'health' of estuarine systems. In order to compute algae and dissolved oxygen, a large suite of model state variables is necessary (Table 1). The phytoplankton kinetics are detailed here. Formulation of the

remaining eutrophication processes is largely as previously described (Cerco ands Cole 1994).

Phytoplankton Kinetics

The model simulates three algal groups. The spring algal group comprises the diatoms that dominate saline waters from January to May. The summer algal group represents the assemblage of flagellates, diatoms and other phytoplankton that dominate the system from May to December. The blue-green algal group represents the *Microcystis* that are found only in the tidal freshwater portion of the Potomac River. Each algal group is represented by identical formulations. Differences between groups are determined by parameter specifications.

For phytoplankton, the sources and sinks in the conservation equation include production, metabolism, predation, and settling. These are expressed:

$$\frac{\Sigma S}{V} = \left(G - BM - W \frac{d}{dz} \right) B - PR \qquad (2)$$

B = algal biomass, expressed as carbon (g C m^{-3})
G = growth (d^{-1})
BM = basal metabolism (d^{-1})
W = settling velocity (m d^{-1})
PR = predation (g C m^{-3} d^{-1})
z = vertical coordinate (m)

Production

Production by phytoplankton is determined by the availability of nutrients, by the intensity of light, and by the ambient temperature.

Light

The influence of light on phytoplankton production is represented by a chlorophyll-specific production equation (Jassby and Platt 1976):

$$P = Pmax \frac{I}{\sqrt{I^2 + Ik^2}} \qquad (3)$$

P = production (gm C gm^{-1} Chl day^{-1})
Pmax = production rate under optimal conditions (gm C gm^{-1} Chl day^{-1})
I = irradiance (E m^{-2} day^{-1})

Parameter Ik is defined as the irradiance at which the initial slope of the production vs. irradiance relationship (Figure 3) intersects the value of Pmax:

$$Ik = \frac{Pmax}{a} \quad (4)$$

a = initial slope of production vs. irradiance relationship (g C g^{-1} Chl E^{-1} m^{-2})

The formulation of production differs from the relations commonly employed in engineering models (e.g. DiToro et al. 1971, Cole and Buchak 1995, Cerco and Cole 1994). Formulations similar to Equation 3 are widely employed in oceanographic models and elsewhere, however. The primary advantage in their use is that Pmax, Ik, and a are commonly measured and reported. Chlorophyll-specific production rate is readily converted to carbon specific growth rate, for use in Equation 3, through division by the carbon-to-chlorophyll ratio:

$$G = \frac{Pmax}{CChl} \quad (5)$$

CChl = carbon-to-chlorophyll ratio (g C g^{-1} chlorophyll a)

Nutrients

Carbon, nitrogen, and phosphorus are the primary nutrients required for algal growth. Diatoms require silica, as well. Inorganic carbon is usually available in excess and is not considered in the model. The effects of the remaining nutrients on growth are described by the formulation commonly referred to as "Monod kinetics" (Monod 1949):

$$f(N) = \frac{D}{KHd + D} \quad (6)$$

f(N) = nutrient limitation on algal production ($0 \leq f(N) \leq 1$)
D = concentration of dissolved inorganic nutrient (g m^{-3})
KHd = half-saturation constant for nutrient uptake (g m^{-3})

Temperature

Algal production increases as a function of temperature until an optimum temperature or temperature range is reached. Above the optimum, production declines until a temperature lethal to the organisms is attained. Numerous functional representations of temperature effects are available. Inspection of growth versus temperature curves indicates a function similar to a Gaussian probability curve provides a good fit to observations:

$$f(T) = e^{-KTg1\,(T - Topt)^2} \text{ when } T \leq Topt$$

$$= e^{-KTg2\,(Topt - T)^2} \text{ when } T > Topt \quad (7)$$

T = temperature (^oC)

Topt = optimal temperature for algal growth (^oC)
KTg1 = effect of temperature below Topt on growth ($^oC^{-2}$)
KTg2 = effect of temperature above Topt on growth ($^oC^{-2}$)

Combining Effects of Light, Nutrients, and Temperature

Phytoplankton models which consider multiple nutrients commonly invoke Leibig's "law of the minimum" (Odum 1971) so that the nutrient limitation on growth is determined by the single most limiting nutrient (Ambrose et al. 1991, Cerco and Cole 1994, Cole and Buchak 1995). This logic is not always extended to incorporate the light limitation, however. Often, the nutrient limitation is multiplied by the light limit (DiToro et al. 1971, Ambrose et al. 1991). As an alternative, Leibig's law can be extended to include light so that the minimum of light or one of three nutrients determines growth limitation. At present, models that functionally combine the effects of light and a single nutrient have been presented (Laws and Chalup 1990; Cloern et al. 1995) but no unifying theory for the effects of light and multiple nutrients exists. In the absence of this theory, extension of Leibig's law to include light seems most rational. That is, it takes a fixed ratio of nutrients and photons to produce a unit of carbon. Production will be limited by whichever one of these is most limiting. Thus, algal production is modeled:

$$P = Pmax \bullet f(T) \bullet \text{minimum} \left(\frac{NH_4 + NO_3}{KHn + NH_4 + NO_3} , \right. \qquad (8)$$

$$\left. \frac{PO_4 d}{KHp + PO_4 d} , \frac{Si}{KHsi + Si} , \frac{I}{\sqrt{I^2 + Ik^2}} \right)$$

NH_4 = ammonium concentration (gm N m^{-3})
NO_3 = nitrate concentration (gm N m^{-3})
KHn = half-saturation concentration for nitrogen uptake (gm N m^{-3})
PO_4d = dissolved phosphate concentration (gm P m^{-3})
KHp = half-saturation concentration for phosphorus uptake (gm P m^{-3})
Si = dissolved silica concentration (gm Si m^{-3})
KHsi = half-saturation concentration for silica uptake (gm Si m^{-3})

Basal Metabolism

Basal metabolism is considered to be an exponentially increasing function of temperature:

$$BM = BMr \ e^{KTb \ (T - Tr)} \qquad (9)$$

BMr = metabolic rate at Tr (d^{-1})
KTb = effect of temperature on metabolism ($^oC^{-1}$)
Tr = reference temperature for metabolism (^oC)

Predation

The predation term includes the computed activity of zooplankton and a term that represents predation by planktivorous fish. Formulation and results of the zooplankton computation may be found in Cerco and Meyers (2000) and Cerco (2000). Predation by fish is modeled by assuming fish clear a specific volume of water per unit biomass:

$$PR = F \bullet B \bullet M \tag{10}$$

F = filtration rate (m^3 g^{-1} fish C day^{-1})
M = fish biomass (gm C m^{-3})

Absent a fisheries model, specification of the spatial and temporal distribution of the predator population is impossible. One approach is to assume fish biomass is proportional to algal biomass, M = g B, in which case Equation 10 can be rewritten:

$$PR = g \bullet F \bullet B^2 \tag{11}$$

Since neither g nor F is known precisely, the logical approach is to combine their product into a single unknown determined during the model calibration procedure. Effect of temperature on predation is represented with the same formulation as the effect of temperature on respiration. The final representation of predation, including zooplankton, is:

$$PR = \frac{B}{KHsz + B} \bullet RMsz \bullet SZ + \frac{B}{KHlz + B} \bullet RMlz \bullet LZ + Phtl \bullet B^2 \tag{12}$$

RMsz = microzooplankton maximum ration (g algal C g^{-1} zoo C d^{-1})
SZ = microzooplankton biomass (g C m^{-3})
KHsz = half saturation concentration for carbon uptake by microzooplankton (g C m^{-3})
RMlz = mesozooplankton maximum ration (gm algal C gm^{-1} zoo C d^{-1})
LZ = mesozooplankton biomass (g C m^{-3})
KHlz = half saturation concentration for carbon uptake by mesozooplankton (g C m^{-3})
Phtl = rate of predation by higher trophic levels (m^3 g^{-1} C d^{-1})

Effect of Algae on Phosphorus

Model phosphorus state variables include total phosphate (dissolved, sorbed, and algal), dissolved organic phosphorus, labile particulate organic phosphorus, and refractory particulate organic phosphorus. The amount of phosphorus incorporated in algal biomass is quantified through a stoichiometric ratio. Thus, total phosphorus in the model is expressed:

$$TotP = PO_4d + PO_4p + Apc\_B + DOP + LPOP + RPOP \quad (13)$$

TotP = total phosphorus (g P m^{-3})
PO_4d = dissolved phosphate (g P m^{-3})
Apc = algal phosphorus-to-carbon ratio (g P g^{-1} C)
PO_4p = particulate inorganic phosphate (g P m^{-3})
DOP = dissolved organic phosphorus (g P m^{-3})
LPOP = labile particulate organic phosphorus (g P m^{-3})
RPOP = refractory particulate organic phosphorus (g P m^{-3})

Algae take up dissolved phosphate during production and release dissolved phosphate and organic phosphorus through respiration. The fate of phosphorus released by respiration is determined by empirical distribution coefficients. The fate of algal phosphorus incorporated by zooplankton and lost through zooplankton mortality is determined by a second set of distribution parameters. Details of these formulations may be found in Cerco and Cole (1994) and Cerco (2000).

Effect of Algae on Nitrogen

Model nitrogen state variables include ammonium, nitrate, dissolved organic nitrogen, labile particulate organic nitrogen, and refractory particulate organic nitrogen. The amount of nitrogen incorporated in algal biomass is quantified through a stoichiometric ratio. Thus, total nitrogen in the model is expressed:

$$TotN = NH_4 + NO_3 + Anc\_B + DON + LPON + RPON \quad (14)$$

TotN = total nitrogen (g N m^{-3})
NH_4 = ammonium (g N m^{-3})
NO_3 = nitrate (g N m^{-3})
Anc = algal nitrogen-to-carbon ratio (g N g^{-1} C)
DON = dissolved organic nitrogen (g N m^{-3})
LPON = labile particulate organic nitrogen (g N m^{-3})
RPON = refractory particulate organic nitrogen (g N m^{-3})

Algae take up ammonium and nitrate during production and release ammonium and organic nitrogen through respiration. Nitrate is internally reduced to ammonium before synthesis into biomass occurs (Parsons et al. 1984). Trace concentrations of ammonium inhibit nitrate reduction so that, in the presence of ammonium and nitrate, ammonium is utilized first. The “preference” of algae for ammonium is expressed by an empirical function (Thomann and Fitzpatrick 1982) with two limiting values (Figure 4). When nitrate is absent, the preference for ammonium is unity.

When ammonium is absent, the preference is zero. In the presence of ammonium and nitrate, the preference depends on the abundance of both forms relative to the half-saturation constant for nitrogen uptake. When both ammonium and nitrate are abundant, the preference for ammonium approaches unity. When ammonium is scarce but nitrate is abundant, the preference decreases in magnitude and a significant fraction of algal nitrogen requirement comes from nitrate.

As with phosphorus, the fate of algal nitrogen released by metabolism and predation is represented by distribution coefficients.

Effect of Algae on Silica

The model incorporates two siliceous state variables: dissolved silica and particulate biogenic silica. The amount of silica incorporated in algal biomass is quantified through a stoichiometric ratio. Thus, total silica in the model is expressed:

$$TotSi = Dsil + Asc\_B + PBS \quad (15)$$

TotSi = total silica (g Si m^{-3})
Dsil = dissolved silica (g Si m^{-3})
Asc = algal silica-to-carbon ratio (g Si g^{-1} C)
PBS = particulate biogenic silica (g Si m^{-3})

As with the other nutrients, the fate of algal silica released by metabolism and predation is represented by distribution coefficients.

Parameter Evaluation

Model parameter evaluation is a recursive process. Parameters are selected from a range of feasible values, tested in the model, and adjusted until satisfactory agreement between predicted and observed variables is obtained. Ideally, observation or experiment determines the range of feasible values. For some parameters, however, no observations are available. Then, the feasible range is determined by parameter values employed in similar models or by the judgement of the modeler. Parameters are reported here for the spring and summer algal groups, which inhabit the mainstem of Chesapeake Bay. Parameters for the blue-green group, modeled only in the tidal fresh Potomac may be found in Cerco (2000).

Algal Production Parameters

Maximum production rates and their temperature dependence were based on observations collected by Harding et al. (1986). The observed production rates were subject to in-situ nutrient limitations. Since the maximum production rates employed by the model are for nutrient-unlimited situations, parameter values (Table 2) were selected to provide an envelope around reported rates (Figure 5) based on the assumption that reported rates represented nutrient-limited conditions.

Initial model runs were conducted using values of a close to mean reported values (Harding et al. 1986), roughly 8 g C g^{-1} Chl E^{-1} m^{-2}. While these values provided satisfactory computations of observed chlorophyll, computations did not agree with conventional wisdom regarding light limitations of algal production in the upper bay (Fisher et al. 1992; Glibert et al. 1995). Consequently, a was adjusted downward until light limitation was initiated in the turbidity maximum. As a result, Ik was substantially higher than reported values (Figure 6).

Basal Metabolism

Tang and Peters (1995) summarized respiration rates measured for six algal divisions in 178 experiments. Respiration reported on a per cell basis varied widely. When normalized by biomass, however, specific respiration demonstrated a relatively narrow range, 0.3 to 0.5 d^{-1}. Respiration rates in this range were used as initial estimates in the model and refined in the calibration procedure. The final value for the summer group, 0.2 d^{-1}, was close to the initial estimate. Final value for the spring group, 0.01 d^{-1}, was much less than the initial estimate but was required to reproduce the elevated chlorophyll concentrations found at great depths during spring. When higher respiration rates were employed, algae expired rather than forming a subsurface chlorophyll maximum. The reference temperature (Tr = 20 ^{o}C) and temperature effect, Ktb = 0.0322 $^{o}C^{-1}$, were taken directly from Tang and Peters (1995).

Predation

Parameters for the zooplankton model have been reported previously (Cerco and Meyers 2000). Parameters for predation by fish were based on information provided in a preliminary bioenergetics model of Atlantic Menhaden (Bartleson et al. 1994). Menhaden enter the bay in spring as larvae and emigrate in fall as juveniles. The bioenergetics model indicated predation by menhaden consumes less than five percent of primary production in mid-Chesapeake Bay. Parameter Phtl was assigned a value, 0.01 m^3 g^{-1} C d^{-1}, such that computed predation was less than five percent of modeled primary production in the mid bay (Figure 7). The predation term was specified at 20 ^{o}C and assumed to double for a 10 ^{o}C increase in temperature. The predation term was activated only from June to October when menhaden are present in the bay.

Composition

Initial estimates of algal stoichiometry were obtained from monitoring data collected by the EPA Chesapeake Bay Program Office. Estimates were based on the assumption that composition of organic particles near the surface of the Bay (depth $\leq$ 2 m) approximates the composition of viable algae. Observations collected in the mainstem bay in 1994 (Figure 12) were employed in the analysis. This year was selected since observations of particulate inorganic phosphorus and particulate biogenic silica were collected as part of a supplemental monitoring program.

Type II linear regression (Ricker 1973; Laws and Archie 1981), appropriate when the value of the independent variable is uncertain, was employed in the determination of all ratios. First, carbon-to-chlorophyll ratio was determined by finding the best fit to the relationship:

$$POC = POCb + CChl \bullet CHL \quad (16)$$

POC = observed particulate organic carbon (g C m^{-3})
POCb = mean value of non-algal POC (g C m^{-3})
CHL = observed chlorophyll (mg Chl `a` m^{-3})

The carbon-to-chlorophyll ratio (Table 3, Figure 8) was used in subsequent regressions to estimate, from the observed chlorophyll, the POC associated with viable algae. For nitrogen, the regression was:

$$PON = PONb + Apn \bullet (CChl \bullet Chl) \quad (17)$$

PON = observed particulate organic nitrogen (gm N m^{-3})
PONb = mean value of non-algal PON (g N m^{-3})

A large fraction of the particulate phosphorus in Chesapeake Bay is in inorganic form (Keefe 1994). Consequently, regression against the particulate phosphorus commonly observed in the monitoring program can lead to spurious results. For phosphorus, observations of particulate inorganic phosphorus were subtracted from corresponding observations of particulate phosphorus to yield estimates of particulate organic phosphorus. Then a regression on a relationship similar to Equation 17 was employed to estimate algal composition (Table 3, Figure 10).

Determination of silica stoichiometry followed similar principles. An initial regression on all data yielded no significant relationship. When only data collected in March and May, during the spring bloom were considered, a significant relationship was obtained (Table 3, Figure 11).

Final values of algal stoichiometry employed in the model (Table 3) were obtained by "tuning" the initial estimates to improve agreement between computed and observed organic carbon, chlorophyll, and nutrients. Model carbon-to-chlorophyll ratios are close to initial estimates and compare well with the ratio 90:1 proposed by Harding et al. (1986) and the mean value 63:1 derived from Malone et al. (1988). Model nitrogen-to-carbon ratios are closer to the classic Redfield ratio (Redfield et al. 1966), 0.176 gm N gm^{-1} C, than the regression value. Model phosphorus-to-carbon ratio is less than both the regression and Redfield stoichiometry (0.019 gm P gm^{-1} C). The model value was selected to optimize the fit of chlorophyll and phosphate during phosphorus-limited conditions such as the spring bloom. Model silica-to-carbon ratio for the spring algal group compares well with both the regression value and the range of values, 0.5 to 1.0 gm Si gm^{-1} C, summarized by Parsons et al. (1984). For the summer group, a much lower ratio was specified since diatoms comprise only a fraction of the summer algal population.

Nutrient Uptake

Reported half-saturation concentrations for algal nutrient uptake in Chesapeake Bay are 0.001 to 0.008 gm N m^{-3} for ammonium (Wheeler et al. 1982) and 0.003 to 0.053 gm P m^{-3} for phosphate (Taft et al. 1975). Both studies comprised a limited number of observations conducted over a

short term. The half-saturation concentrations reported by Wheeler et al. (1982) are much less than the range of values commonly reported for neritic phytoplankton. Means of values summarized by Eppley et al. (1969) are in the range 0.028 to 0.052 g N m^{-3}, depending on substrate composition and plankton division. Corresponding model values are 0.03 gm N m^{-3} and 0.003 gm P m^{-3} (spring group) and 0.025 gm N m^{-3} and 0.001 gm P m^{-3} (summer group). Summer values were specified smaller than spring values since the cell size of the pico-nanoplankton complex that dominates in summer (Marshall and Lacouture 1986) is smaller than the spring diatom group. Concentrations specified in the model closely reflect the reported summaries (Eppley et al. 1969) for nitrogen and are at or below the lowest values for phosphorus reported by Taft et al. (1975).

The model half-saturation concentration for silica uptake by spring diatoms, 0.05 g Si m^{-3}, is well within reported values, 0.02 to 0.082 g Si m^{-3}, for oceanic diatoms (Davis et al. 1978; Parsons et al. 1984). The half saturation concentration for the summer group, 0.01 g Si m^{-3}, was specified to prevent silica limitation from occurring during this season.

Algal Settling Rates

Reported algal settling rates typically range from 0.1 to 5 m d^{-1} (Bienfang et al.1982; Riebesell 1989; Waite et al. 1992). In part, this variation is a function of physical factors related to algal size, shape, and density (Hutchinson 1967). The variability also reflects regulation of algal buoyancy as a function of nutritional status (Bienfang et al. 1982; Richardson and Cullen 1995) and light (Waite et al. 1992). Under appropriate conditions, diatoms exhibit ascent rather than settling (Moore and Villareal 1996) while dinoflagellates are capable of vertical migration both upwards and downwards (Eppley et al. 1968; Heaney and Eppley 1981). The algal settling rate employed in the model represents the net effect of all physiological and behavioral processes that result in downward transport of phytoplankton. The settling rate employed, 0.1 m d^{-1}, was derived through tuning of observed chlorophyll and nutrient concentrations.

Distribution of Algal Carbon and Nutrients

Carbon, nitrogen, phosphorus, and silica released to the environment through algal metabolism and through predation on algae must be routed into appropriate model state variables. For carbon, these are dissolved, labile particulate, and refractory particulate organic forms. For nitrogen and phosphorus, a dissolved inorganic fraction must be specified as well as organic fractions. For silica, the splits are between dissolved silica and particulate biogenic silica.

A number of studies (Table 4) have incubated algae and algal detritus to examine the products and rate of decomposition. Direct relation of experimental observations to the model is difficult since the experiments were not designed to measure distribution as parameterized in the model. No universal distinction between labile and refractory exists. Definition in the present study was based on parameters employed in the sediment diagenesis model (DiToro and Fitzpatrick 1993). In the sediment model, the carbon fraction deemed labile (G1) had a decay rate of 0.035 day^{-1} @ 20 ^{o}C. Ninety-percent of G1 carbon was mineralized in 65 days. In interpretation of experiments, organic matter that mineralized in . 60 days or less was considered labile.

Aspects of carbon and nutrient release from zooplankton have been studied (e.g. Morales 1987; Wen and Peters 1994; Miller et al. 1995) but this material does not readily allow the apportionment of total consumption into releases in organic, inorganic, dissolved and particulate form. Recycling of algal matter back to the water by fish must also be parameterized in some fashion. Ultimately, the splits of carbon and nutrients released by algal metabolism and by predation (Table 5) were determined by adjustment to agree with observed concentrations.

Results

Model simulations encompassed the period 1985-1994. The ten-year simulation was continuous, employing fifteen-minute time steps. Intra-tidal hydrodynamics for each of the ten years were provided by the CH3D-WES hydrodynamic model (Johnson et al. 1993) operating on the 10196-cell grid (Figure 2). Loads from the watershed were provided on a daily basis by a current version of the EPA's Chesapeake Bay Watershed Model (Donigian et al. 1991). Point-source loads were specified monthly based on reports from state agencies. Atmospheric loads to the water surface were derived from observations and specified on a daily basis.

Chlorophyll, carbon, nutrients and other substances are monitored at over fifty stations (Figure 12) in the mainstem of Chesapeake Bay. Surveys are conducted at monthly or greater frequencies and samples are collected at four or more depths in the water column. The enormous quantity of data provides both an opportunity and a challenge in model-data comparisons. Some degree of spatial and temporal aggregation is necessary to reduce the volume of information into a representative assembly.

Spatial Distribution of Phytoplankton and Nutrients

One aggregation employed in the study compared model and data along a transect extending from the mouth of the bay to the head of tide at the Susquehanna River. The ten-year simulation period was divided into three intervals: 1985-1988, 1989-1992, 1993-1994. The first interval corresponded to the period prior to major phosphorus load controls. The second period encompassed phosphorus controls under years of average hydrology. The last two years represented unusually high runoff in the Susquehanna. Years were divided into seasons of three months each. Seasonal medians of observed and modeled concentrations were computed for four seasons in each of the three intervals. These comparisons provided a broad indication of the model's ability to represent the spatial distribution of phytoplankton, nutrients, and other substances. Two seasons are shown here: spring (March-May) and summer (June-August) 1989-1992. These seasons were selected to illustrate computations of the spring algal bloom and the summer period of maximum production. Results are shown for chlorophyll and the quantities that influence chlorophyll distribution: ammonium, nitrate, phosphate, silica, and light attenuation.

Spring

Median observed chlorophyll concentrations during spring (Figure 13) were 5 to 10 mg m^{-3} with a tendency for higher concentrations to occur in the upper half of the bay. The model provides

good representation of the magnitude and distribution of surface chlorophyll. Observations indicate chlorophyll concentrations similar to surface values occur at the bottom of the water column. Modeled concentrations are roughly half of surface values throughout much of the bay.

Surface ammonium observations exhibit a peak in the upper part of the bay and are otherwise at trace concentrations. Surface nitrate observations demonstrate a substantial gradient from the gm m^{-3} range at the Susquehanna down to trace concentrations at the mouth of the bay. The magnitude of observed ammonium in the upper bay is well represented in the model although computed ammonium in the lower bay is roughly twice the observed values. Both the magnitude and spatial trends of the observed nitrate are reproduced in the model.

Dissolved inorganic phosphorus observations demonstrate little spatial variation. In much of the bay, they are at or below detection levels. Observations suggest higher values in the turbid waters at the head of the bay and, perhaps at the mouth of the bay. Observations of higher values there are confused, however, by a higher detection levels in samples from that region. The model clearly exhibits a trend to higher concentrations towards the bay mouth and little change in phosphate in the turbidity maximum.

As with nitrate, computed and observed dissolved silica exhibit order-of-magnitude variation from the Susquehanna River source to the mouth of the bay. Concentrations are in the gm m^{-3} range at the Susquehanna outfall yet depleted in the lower 150 km of the bay.

Observed light attenuation is highest in the turbidity maximum in the upper bay. Elsewhere, attenuation is roughly uniform. Light attenuation in the model is computed as a function of computed solids concentration and specified color (Cerco and Meyers 2000). The model reproduces both peak attenuation in the turbidity maximum and the lower, uniform values elsewhere.

Summer

Median observed surface chlorophyll concentrations during summer (Figure 14) were in the 5 to 10 mg m^{-3} range, similar to spring. The primary difference from spring is the absence of chlorophyll in bottom waters, except in the shallowest region near the head of tide. The magnitude of surface chlorophyll concentration and the absence of chlorophyll in bottom waters are well represented in the model.

As with spring, observed surface ammonium exhibits a peak in the turbid reaches of the upper bay and descends to trace concentrations elsewhere. Nitrate again shows enormous variation between the Susquehanna River and the mouth of the bay. In contrast to spring, however, the supply of nitrate from the Susquehanna is depleted in the lower two thirds of the bay. During spring, nitrate was detectable almost to the mouth of the bay. The magnitude and trends of both inorganic nitrogen forms are reproduced in the model.

During summer, observed phosphate exhibits peak values at the mouth of the bay and in turbid waters of the upper bay. In the central portion of the bay, phosphate is at or below detection

levels. The model reproduces the higher concentrations near the bay mouth and the depletion in the central portion of the bay but shows no tendency to increase in the upper bay.

During summer, both computed and observed silica are plentiful in surface waters. As with spring, computed and observed light attenuation are highest in the turbidity maximum and nearly uniform elsewhere.

Temporal Distribution of Phytoplankton and Nutrients

The temporal distribution of chlorophyll, nutrients, and light (Figure 15) are shown at Station CB5.2, located nearly at the center of the bay. The primary feature of the observed chlorophyll time series is the occurrence of the spring bloom with concentrations over 25 mg m^{-3} in both surface and bottom waters. Compressed into a ten-year time series, the bloom can be difficult to discern in surface observations but the subsurface chlorophyll maximum is easy to see in the bottom observations. Modeled surface chlorophyll exhibits both a spring bloom and a secondary summer peak associated with maximum productivity. Relative magnitudes of the two peaks and the duration of the interval between them depends on meteorology and hydrology of the simulated year. The difference between the bloom and subsequent summer period is clearly discerned in the modeled bottom chlorophyll concentration although the model substantially under-computes the magnitude of the subsurface chlorophyll maximum.

Temporal structure in the observed surface ammonium is difficult to discern. The primary feature is the depletion that often occurs in the third quarter of the year. More temporal structure is evident in the nitrate observations which show peaks associated with spring runoff events and nitrate depletion during summer intervals of low flow. Magnitude of the observed concentrations are well reproduced and the model also exhibits depletion of inorganic nitrogen forms in summer.

As with ammonium, observed dissolved phosphate shows little temporal structure in the surface waters of the central bay. Modeled phosphate is of the correct magnitude during spring when diatom uptake is substantial. Otherwise, modeled concentrations are substantially higher than observed.

Observed dissolved silica exhibits a strong seasonal pattern that is out of phase with runoff events. Observed silica is usually least during spring, when diatom uptake is large. Following the spring bloom, silica concentrations increase, despite the low volume of runoff. Concentrations fluctuate but remain at relatively high levels until the subsequent spring bloom period. Magnitude and temporal trends in dissolved silica are well reproduced in the model.
Temporal structure is also difficult to observed in the light attenuation observations. The primary phenomenon, observable in both observations and model, is the occurrence of runoff events which introduce large solids loads and carry these loads down the bay past the usual location of the turbidity maximum. These events are especially prominent in the high-flow years 1993 and 1994.

Light and Nutrient Limitations

The nature and degree of nutrient limitations in the mainstem bay vary with season and location.

One prime determinant is runoff from the Susquehanna River. River runoff is highly enriched in nitrogen relative to algal requirements. Consequently, in spring, when runoff is high, phosphorus and silica tend to be more limiting than nitrogen (Fisher et al. 1992; Malone et al. 1996). During summer, when runoff is low and oceanic water intrudes up the bay, and when internal nutrient recycling provides a substantial portion of algal nutrient requirements, nitrogen is the most limiting nutrient (Fisher et al. 1992; Malone et al. 1996).

Since the estuary transitions from nearly oceanic conditions at the mouth to freshwater at its extreme upstream limit, nutrient limitations also show a spatial trend with phosphorus more limiting at the freshwater extreme and nitrogen and silica more limiting near the mouth (Glibert et al. 1995). Location is also the most important determinant of the relative importance of light relative to nutrient limitations. The bay exhibits a persistent turbidity maximum near the head of salt intrusion (Schubel 1968) and light can be more limiting than nutrients in this region (Fisher et al. 1992; Glibert et al. 1995).
Computed limitations to algal growth are shown at three locations in the bay: Station CB2.2 located near the turbidity maximum, Station 5.2 in the center of the bay, and Station 7.3 located near the bay entrance (Figure 12). Limits are shown for the year 1990 which was a year of average runoff in the Susquehanna River. Although limiting factors respond to annual hydrology and loads, results shown here are largely generalizable across the simulation. Limiting factors are restricted in magnitude from zero to unity (Equation 8). The factor with the lowest value is most limiting.

At the upper bay station, light is the predominant limiting factor although, during the height of the spring bloom, phosphorus limitation occurs (Figure 16). Near the center of the bay, growth limits exhibit seasonal dependence (Figure 17). During the winter months (December-February) light is most limiting. As the days grow longer and the spring bloom commences, phosphate and silica become the most limiting factors. At the end of the spring bloom, the limiting nutrient transitions to nitrogen which limits until the early winter light limit commences.

Limits at the lower bay station resemble the middle bay although the winter light limitation is of shorter duration. During the spring bloom, silica predominates over phosphate as the limiting nutrient while nitrogen is most limiting from late spring through autumn.

Model computations agree well with conventional wisdom regarding spatial and temporal distribution of limiting factors. In the model, phosphate and silica are most limiting in spring while nitrogen is most limiting in summer. Computed light and phosphate limits are dominant in the upper bay while nitrogen and silica limits are dominant in the lower bay.

Primary Production

Primary production is the fixation of carbon dioxide by photosynthesis. Substantial variation exists in techniques to measure and report algal production. Production can be measured in-situ or in vivo, as carbon uptake or as oxygen evolution. Production is alternately reported on a volumetric or areal basis. Techniques and reporting influence the methods for comparison of computed and observed values. For comparison with the model, one important factor is to

differentiate between gross production and net production. Gross production is the rate of carbon fixation; net production is carbon fixation less algal respiration losses. On a volumetric basis, gross production in the present model is:

$$GPP = \frac{Pmax}{CChl} \bullet f(T) \bullet \text{minimum} \left(\frac{D}{KHd + D} , \frac{I}{\sqrt{I^2 + Ik^2}} \right) \bullet B \qquad (18)$$

GPP = gross primary production (g C m^{-3} d^{-1})

Modeled net primary production, NPP, is the gross minus metabolism computed by Equation 9. Production on an areal basis is computed by integration of the volumetric rates over an appropriate depth.

Primary Production Measures in Chesapeake Bay

Measures of primary production were collected by Harding et al. (1986) as part of the same study that provided production parameters for this model. Between March 1982 and April 1983, measures were collected at stations (Figure 19) grouped below the Susquehanna River mouth, in the reach from the Chester to Choptank Rivers, and in the reach from the Potomac to Rappahannock River mouths. Simulated in-situ incubations were conducted on-deck, four times daily, using the ^{14}C method. Measures were integrated over the depth of the pycnocline or the depth of the photic zone, whichever was greater, and reported as net production.

Malone et al. (1988) conducted primary production measures at a transect located opposite the mouth of the Choptank River (Figure 19). The ^{14}C method was employed in 24-hour on deck incubations conducted over a two-year period, 1985-1986. The 24-hour incubations provided estimates of net productivity in the photic zone.

Primary production measures collected from 1990 to 1992 at three locations in the bay (Figure 19) were reported by Kemp et al. (1997). Production was measured via oxygen evolution and consumption in light and dark bottles. Incubations were conducted on deck, at multiple light levels, for a period of four to five hours. Measures were corrected for respiration and reported as gross primary production.

Comparison with Observations

For comparison with the Harding et al. (1986) observations, model net primary production was integrated over the depth of the photic zone. The photic zone was defined as the depth of 1% light penetration, based on light attenuation as computed within the model. Observations were compared to computations in the model years closest to the observations, 1985-1986. In the upper bay (Figure 20), observed and modeled primary production are in reasonable agreement. Maximum observed production, roughly 0.8 gm C m^{-2} d^{-1} compared to a modeled maximum of 1.2 gm C m^{-2} d^{-1}. A deterministic relation of observations to temperature cannot be discerned

although, clearly, primary production as measured at temperature exceeding 10 ^{o}C exceeds primary production measured at lower temperatures. The model exhibits a general exponential dependence of primary production on temperature with maxima occurring in a broad band between 15 and 25 ^{o}C.

Monotonic temperature dependence is absent from the observations collected near the Chester and Choptank Rivers (Figure 21). Primary production peaks were observed during the spring bloom period at 6 ^{o}C and during the summer period of maximum temperatures. Modeled production again showed a dependence on temperature. Maximum modeled production was substantially lower than observed.

Observed primary production in the mid to lower bay (Figure 22) exhibited a U-shaped dependence on temperature. Maximum production occurred at the coldest temperature, during the spring bloom. Elevated production also was observed during summer at temperatures of 15 to 25 ^{o}C. The model clearly replicated the U-shaped temperature function and the magnitude of observed primary production although the modeled maximum occurred in summer, not spring.

The observations of Malone et al. (1988) demonstrated strong inter-annual variability in primary production. In 1985, maximum production occurred in August - October. Maximum production was lower in 1986 and occurred earlier in the summer. Maximum observations, roughly 4.5 g C m^2 d^{-1}, were substantially higher than maxima observed by Harding et al. (1986) in the same area. For comparison with this data set, model net primary production was again integrated over the depth of the photic zone. Model values agree with data in the winter spring period, February - May but fall short of observations in June - December (Figure 23).

Kemp et al. (1997) combined their observations from three years into annual time series at three stations. For comparison, model gross production from 1990-1992 was averaged into annual time series at corresponding locations. At the upper bay station (Figure 24), modeled gross production exhibited the same temproal behavior as observations but was twice as large. In the middle bay and lower bay, modeled production was in reasonable agreement with observations in the period October through March but was short of observed rates from April through August (Figures 25, 26).

Discussion

The present model results are the product of over 170 simulations. In each, model parameters or forcing functions were adjusted in an attempt to optimize comparisons of computed and observed chlorophyll, carbon, nutrients, and dissolved oxygen. A single, optimal calibration can never be obtained. The final results of the model represent the judgement of the modeler in balancing computations of various substances in regions and periods of interest.

Observations (Figures 13, 14) suggest that the light limitation in the turbidity maximum around km 280 is more severe than computed in the model. The model parameter a, which determines light sensitivity, can readily be adjusted to produce greater light limitation in the turbidity maximum. Under these circumstances, computed ammonium and phosphate increase providing

improved agreement with observations. Elsewhere in the system, however, the light limit becomes exaggerated. Consequently, a was specified to provide a reasonable representation of light limitation systemwide.

The high computed phosphate concentrations (Figure 15) can be countered by increasing the phosphorus content of algal cells, APC. Increasing APC promotes too great a phosphorus limit at other times of the year, however. Consequently, APC was specified to correctly represent phosphate during spring, when reports indicate phosphorus limitation is most significant.
The accomplishments of the present study should not be under-estimated. Decade-long, continuous, system-wide simulations were performed on a routine basis. The simulations of eutrophication processes were coupled to detailed, three-dimensional hydrodynamics computed at five-minute intervals. Loads from a 166,000 km^2 watershed were routed to the headwaters and shores of the bay. Over 10^6 observations were processed for comparison with the model. The comparisons indicate largely excellent agreement between computed chlorophyll, nutrients and other substances.

Although different results are possible, the chances of substantially improved results from the present formulation are slim. Consequently, it's worth examining where the model falls short and considering the possibility of improved formulations.

The magnitude of the spring subsurface chlorophyll maximum has been under-computed since the earliest phases of this study. Although more-or-less successful computations have been obtained by varying settling velocities and respiration rates, clearly something is missing from the model. Most likely, the ability of diatoms to regulate their buoyancy (Bienfang et al. 1982; Richardson and Cullen 1995; Waite et al. 1992). At present, algae are represented as passive particles that can only settle. Creation of localized aggregations is discouraged by vertical diffusion which moves algae against the concentration gradient. Although the treatment of algae as Lagrangian particles with individual behaviors is a long way off, insertion of processes into the model that simulate phytoplankton behavior as a function of light and nutrients should be possible.

The earliest version of this model incorporated an empirical representation of variable algal phosphorus stoichiometry (Cerco and Cole 1994). The iterative algorithm was computationally burdensome and dropped from the formulation. Since then, advances have been made in the formulation of phytoplankton models that compute both variable carbon-to-chlorophyll and nitrogen-to-chlorophyll ratios (Laws and Chalup 1990; Cloern et al. 1995). Although a complete model of algal composition as a function of temperature, light, and nutrients is not available, introduction of available formulations will begin to address some of the problems encountered in this study. Computation of carbon-to-chlorophyll ratio as a function of light may balance the light limitation between the turbidity maximum and other regions of the bay. Re-introduction of variable stoichiometry, computed from sound principles, will help balance the computation of phosphate throughout the seasons.

The present model was calibrated to 'states' of the system. That is, parameters were adjusted to optimize agreement between computed and observed concentrations. No attempt was made to examine computed rates of production or recycling. Subsequent comparisons of computed and

observed primary production indicated the model was only partially successful in reproducing this key rate. Comparisons were most successful in the upper bay (Figures 20, 24) and during winter and early spring (Figures 23, 25, 26). Production in the turbidity maximum and in winter-spring is largely light limited. In regions and periods in which production is strongly nutrient limited, the model under-computes primary production (Figures 21, 23, 25, 26).

Computed and observed primary production compare well in turbid, nutrient-rich portions of the bay and during winter when productivity is low. When observed production is maximal and strongly nutrient-limited, computations tend to be low. One question is whether this behavior is unique to the present model or characteristic of a range of similar models. While model studies that examine sensitivity of primary production to various factors are plentiful, models that explicitly compare computed and observed primary production are difficult to find. When the search is narrowed to models that compute both nutrient and light effects on primary production, the field gets narrower still.

Fasham et al. (1990) applied a model that included phytoplankton, zooplankton, bacteria and nutrients to ocean Station 'S' near Bermuda. They calibrated their model to match observed primary production. Their simulations "greatly overestimated the phytoplankton biomass in the summer and autumn." Their results are the inverse of the present model. In Chesapeake Bay, summer phytoplankton biomass is well represented but primary production is underestimated. At Station 'S' summer primary production was matched but phytoplankton biomass was overestimated.

Doney et al. (1996) modeled phytoplankton, zooplankton, and nutrients near Bermuda also. The preponderance of primary production observations exceeded computed rates. They noted model performance was weakest "during late summer, when the model cannot supply enough nutrients to support the high production observed."

The results of McGillicuddy et al. (1995) are especially interesting. They showed computed and observed vertical profiles of primary production in the North Atlantic. In ten of thirteen cases, primary production was under-computed at the surface, where light is abundant and nutrients are scare. In deeper waters, where light is attenuated and nutrients are more abundant, model-data comparisons were much improved. Their results were analogous to the present model in which production is matched or exceeded in light-limited regions but not in nutrient-limited regions.

If the results obtained here are widely applicable, the first question is: Why? One response is the relation

$$GPP = \frac{Pmax}{CChl} \bullet f(T) \bullet \frac{D}{KHd + D} \bullet B \qquad (19)$$

that applies under nutrient-limited conditions is not appropriate. Changes in algal carbon-to-chlorophyll ratio in response to nutrient-limited conditions are well-documented (e.g. Laws and Bannister 1980; Riemann et al. 1989). Cloern et al. (1995) compared algal growth rates

computed with alternate model formulations. One model explicitly accounted for nutrient effects on carbon-to-chlorophyll ratio. The second model formulation was identical to the present one. Computed growth rate with the first model was often substantially higher than with the second model. The greatest differences, however, were under conditions of low light and high nutrients. Under strongly nutrient-limited conditions, differences in the two models were not substantial.

A second possibility is that the present production formulations are appropriate but some behavioral process is missing. Heaney and Eppley (1981) noted that vertical migrations of dinoflagellates were influenced by nutrient status and that nutrient-depleted cells appear to migrate towards the oceanic nitracline. Moore and Villareal (1996) observed vertical migration of oceanic diatoms and indicated this migration is a source of nitrogen to the euphotic zone. These results suggest that the model formulation in which algae are influenced solely by nutrient concentrations in their local cell require revision. The spacing of cells in the vertical is a construct required to model vertical density structure. If algae are capable of migrating vertically, then perhaps algal concentrations and available nutrients should be averaged over a length scale that describes the extent of their migrations.

Another question is: "Does the underestimation of primary production matter?" The answer is: "It depends on the objective of the model." The present model construct provides excellent comparisons of computed and observed algal biomass and of the factors that limit biomass. If the objective of a model study is to compute algal biomass and to investigate the management of biomass through nutrient controls, the present construct is adequate. If the objective of a model is to reproduce the carbon cycle or to investigate the transfer of production from primary producers to high trophic levels, then the present construct requires revision.

Acknowledgments

Development of the Chesapeake Bay model package was sponsored by the U.S. Army Engineer District, Baltimore, and the Chesapeake Bay Program Office, U.S. Environmental Protection Agency. Permission was granted by the Chief of Engineers to publish this information.

References

Ambrose, R., Wool, T., Martin, J., Connolly, J., and Schanz, R. (1991). "WASP4, a hydrodynamic and water quality model - model theory, user's manual, and programmer's guide," Environmental Research Laboratory, Office of Research and Development, US Environmental Protection Agency, Athens GA.

Bartleson, R., Boynton, W., Brandt, S., Hagy, J., Hartman, K., Kemp, W., Luo, J., Madden, C., Meyers, M., Rippetoe, T., and Wetzel, R. (1994). "Chesapeake Bay ecosystem modeling program technical synthesis report 1993-1994," US Environmental Protection Agency Chesapeake Bay Program Office, Annapolis MD.

Bienfang, P., Harrison, P., and Quarmby, L. (1982). "Sinking rate respone to depletion of nitrate, phosphate, and silicate in four marine diatoms," *Marine Biology*, 67, 295-302.

Boynton, W., and Kemp, W. (1985). “Nutrient regeneration and oxygen consumption along an estuarine salinity gradient,” *Marine Ecology Progress Series*, 23, 45-55.

Cerco, C. (1995a). “Response of Chesapeake Bay to nutrient load reductions,” *Journal of Environmental Engineering*, 121(8), 549-557.

Cerco, C. (1995b). “Simulation of long-term trends in Chesapeake Bay eutrophication,” *Journal of Environmental Engineering*, 121(4), 298-310.

Cerco, C., and Meyers, M. (2000). “Tributary refinements to the Chesapeake Bay Model,” *Journal of Environmental Engineering*, in press.

Cerco, C. (2000). “Tributary Refinements to Chesapeake Bay Environmental Model Package Part I: Kinetics.” *Technical Report EL-00-xx*, US Army Corps of Engineers Waterways Experiment Station, Vicksburg MS

Cerco, C., and Cole, T. (1993). “Three-dimensional eutrophication model of Chesapeake Bay,” *Journal of Environmental Engineering*, 119(6), 1006-10025.

Cerco, C., and Cole, T. (1994). “Three-dimensional eutrophication model of Chesapeake Bay,” Technical Report EL-94-4, U.S. Army Engineer Waterways Experiment Station, Vicksburg, MS.

Cloern, J., Grenz, C., and Vidergar-Lucas, L. (1995). “An empirical model of the phytoplankton chlorophyll:carbon ratio - the conversion factor between productivity and growth rate,” *Limnology and Oceanography*, 40(7), 1313-1321.

Cole, T., and Buchak, E. (1995). “CE-QUAL-W2: a two-dimensional, laterally averaged, hydrodynamic and water quality model, version 2.0,” Instruction Report EL-95-1, US Army Engineer Waterways Experiment Station, Vicksburg, MS.

Davis, C., Breitner, N., and Harrison, P. (1978). "Continuous culture of marine diatoms under silicon limitation. 3. a model of Si-limited diatom growth," *Limnology and Oceanography*, 23, 41-52.

DiToro, D., O'Connor, S., and Thomann, R. (1971). “A dynamic model of the phytoplankton population in the Sacramento-San Joaquin Delta,” *Nonequilibrium systems in water chemistry*, American Chemical Society, Washington, DC, 131-180.

DiToro, D., and Fitzpatrick, J. (1993). “Chesapeake Bay sediment flux model,” Contract Report EL-93-2, US Army Engineer Waterways Experiment Station, Vicksburg, MS.

Doney, S., Glover, D., and Najjar, R. (1996), “A new coupled, one-dimensional biological-physical model for the upper ocean: Applications to the JGOFS Bermuda Atlantic Time-series Study (BATS) site,” *Deep Sea Research II*, 43(2-3), 591-624.

Donigian, A., Bicknell, B., Patwardhan, A., Linker, L., Alegre, D., Chang, C., and Reynolds, R. (1991). "Watershed model application to calculate bay nutrient loadings," Chesapeake Bay Program Office, US Environmental Protection Agency, Annapolis, MD.

Dortch, Q. (1990). “The interaction between ammonium and nitrate uptake in phytoplankton” *Marine Ecology Progress Series*, 61, 183-201.

Eppley, R., Holm-Hansen, O., and Strickland, J. (1968). “Some observations on the vertical migration of dinoflagellates,” *Journal of Phycology*, 4, 333-340.

Eppley, R., Rogers, J., and McCarthy, J. (1969). “Half-saturation constants for uptake of nitrate and ammonium by marine phytoplankton,” *Limnology and Oceanography*,” 14(6), 912-920.

Fasham, M., Ducklow, H., and McKelvie, S. (1990). “A nitrogen-based model of plankton dynamics in the oceanic mixed layer,” *Journal of Marine Research*, 48, 591-639.

Fisher, T., Peele, E., Ammerman, J., and Harding, L. (1992). “Nutrient limitation of phytoplankton in Chesapeake Bay,” *Marine Ecology Progress Series*, 82,51-63.

Foree, E., and McCarty, P. (1970). "Anaerobic decomposition of algae," *Environmental Science and Technology*, 4, 842-849.

Garber, J. (1984). "Laboratory study of nitrogen and phosphorus remineralization during the decomposition of coastal plankton and seston," *Estuarine, Coastal and Shelf Science*, 18, 685-702.

Glibert, P., Conley, D., Fisher, T., Harding, L., and Malone, T. (1995). “Dynamics of the 1990 winter/spring bloom in Chesapeake Bay,” *Marine Ecology Progress Series*, 122, 27-43.

Grill, E., and Richards, F. (1964). "Nutrient regeneration from phytoplankton decomposing in seawater," *Journal of Marine Research*, 22, 51-69.

Harding, L., Meeson, B., and Fisher, T. (1986). “Phytoplankton production in two east coast estuaries: photosynthesis-light functions and patterns of carbon assimilation in Chesapeake and Delaware bays,” *Estuarine, Coastal and Shelf Science*, 23, 773-806.

Heaney, S., and Eppley, R. (1981). “Light, temperature and nitrogen as interacting factors affecting diel vertical migrations of dinoflagellates in culture,” Journal of Plankton Research, 3(2), 331-344.

Hutchinson, G. (1967). *A treatise on limnology*, *Volume II*, John Wiley & Sons, New York, 245-305.

HydroQual. (1987). “A steady-state coupled hydrodynamic/water quality model of the eutrophication and anoxia process in Chesapeake Bay,” Final Report, HydroQual Inc., Mahwah,

NJ.

Jassby, A., and Platt, T. (1976). “Mathematical formulation of the relationship between photosynthesis and light for phytoplankton,” *Limnology and Oceanography*, 21, 540-547.

Johnson, B., Kim, K., Heath, R., Hsieh, B., and Butler, L. (1993). “Validation of a three-dimensional hydrodynamic model of Chesapeake Bay,” *Journal of Hydraulic Engineering*, 199(1), 2-20.

Keefe, C. (1994). "The contribution of inorganic compounds to the particulate carbon, nitrogen, and phosphorus in suspended matter and surface sediments of Chesapeake Bay," *Estuaries*, 17(1B), 122-130.

Kemp, W., Smith, E., DiPasquale, M., and Boynton, W. (1997). “Organic carbon balance and net ecosystem metabolism in Chesapeake Bay,” *Marine Ecology Progress Series*, 150, 229-248.

Laws, E., and Archie, J. (1981). "Appropriate use of regression analysis in marine biology," *Marine Biology*, 65, 13-16.

Laws, E., and Chalup, M. (1990). “A microalgal growth model,” *Limnology and Oceanography*, 35(3), 597-608.

Leonard, B. (1979). “A stable and accurate convection modelling procedure based on quadratic upstream interpolation,” *Computer Methods in Applied Mechanics and Engineering*, 19, 59-98.

Malone, T., Crocker, L., Pike, S., and Wendler, B. (1988). “Influences of river flow on the dynamics of phytoplankton production in a partially stratified estuary,” *Marine Ecology Progress Series*, 48, 235-249.

Malone, T., Conley, D., Fisher, T., Gliert, P., Harding, L., and Sellner, K. (1996). “Scales of nutrient-limited phytoplankton productivity in Chesapeake Bay,” *Estuaries*, 19(2B), 371-385.

Marshall, H., and Lacouture, R. (1986). “Seasonal patterns of growth and composition of phytoplankton in the lower Chesapeake Bay and vicinity,” *Estuarine, Coastal and Shelf Science*, 23, 115-130.

Miller, C., Penry, D., and Glibert, P. (1995). “The impact of trophic interactions on rates of nitrogen regeneration and grazing in Chesapeake Bay,” *Limnology and Oceanography*, 40(5), 1005-1011.

Monod, J. (1949). “The growth of bacterial cultures,” *Annual Review of Microbiology*, 3, 371-394.

McGillicuddy, D., McCarthy, J., and Robinson, A. (1995). “Coupled physical and biological modeling of the spring bloom in the North Atlantic (I): model formulation and one dimensional

bloom processes," *Deep Sea Research I*, 42(8), 1313-1357.

Moore, J., and Villareal, T. (1996). "Size-ascent relationships in positively buoyant marine diatoms," *Limnology and Oceanography*, 41(7), 1514-1520.

Morales, C. (1987). "Carbon and nitrogen content of copepod faecal pellets: effect of food concentration and feeding behavior," *Marine Ecology Progress Series*, 36, 107-114.

Odum, E. (1971). *Fundamentals of Ecology*, 3rd ed., W. B. Saunders, Philadelphia, PA, 106-107.

Otsuki, A., and Hanya, T. (1972). "Production of dissolved organic matter from dead green algal cells. I. aerobic microbial decomposition," *Limnology and Oceanography*, 17, 248-257.

Parsons, T., Takahashi, M., and Hargrave, B. (1984). *Biological oceanographic processes, 3rd ed.*, Pergamon Press, Oxford.

Pett, R. (1989). "Kinetics of microbial mineralization of organic carbon from detrital *Skeletonema Costatum* cells," *Marine Ecology Progress Series*, 52, 123-128.

Pritchard, D. (1967). "Observations of circulation in coastal plain estuaries." *Estuaries*. G. Lauff ed., American Association for the Advancement of Science, Washington, 37-44.

Redfield, A., Ketchum, B., and Richards, F. (1966). "The influence of organisms on the composition of sea-water." *The Sea Volume II*. Interscience Publishers, New York, 26-48.

Richardson, T., and Cullen, J. (1995). "Changes in buoyancy and chemical composition during growth of a coastal marine diatom: ecological and biogeochemical consequences," *Marine Ecology Progress Series*, 128, 77-90.

Ricker, W. (1973). "Linear regressions in fishery research," *Journal of the Fisheries Research Board of Canada*, 30, 409-434.

Riebesell, U. (1989). "Comparison of sinking and sedimentation rate measurements in a diatom winter/spring bloom," *Marine Ecology Progress Series*, 54, 109-119.

Riemann, B., Simonsen, P., and Stensgaard, L. (1989). "The carbon and chlorophyll content of phytoplankton from various nutrient regimes," *Journal of Plankton Research*, 11(5), 1037-1045.

Schubel, J. (1968). "Turbidity maximum of the northern Chesapeake Bay," *Science*, 161, 1013-1015.

Taft, J., Taylor, W., and McCarthy, J. (1975). "Uptake and release of phosphorus by phytoplankton in the Chesapeake Bay estuary, USA," *Marine Biology*, 33, 21-32.

Tang, E., and Peters, R. (1995). "The allometry of algal respiration," *Journal of Plankton*

Research, 17(2), 303-315.

Thomann, R., and Fitzpatrick, J. (1982). “Calibration and verification of a mathematical model of the eutrophication of the Potomac Estuary,” HydroQual Inc., Mahwah, NJ.

Waite, A., Thompson, P., and Harrison, P. (1992). “Does energy control the sinking rates of marine diatoms?.” *Limnology and Oceanography*, 37(3), 468-477.

Wen, Y., and Peters, R. (1994). “Empirical models of phosphorus and nitrogen excretion by zooplankton,” *Limnology and oceanography*, 39(7), 1669-1679.
Westrich, J., and Berner, R. (1984).”The role of sedimentary organic matter in bacterial sulfate reduction: the G model tested,” *Limnology and Oceanography*, 29, 236-249.

Wheeler, P., Gilbert, P., and McCarthy, J. (1982). “Ammonium uptake and incorporation by Chesapeake Bay phytoplankton: short-term uptake kinetics,” *Limnology and Oceanography*, 27, 1113-1128.

List of Figures

Table 1
Water Quality Model State Variables

Temperature	Salinity
Inorganic Suspended Solids	Freshwater Cyanobacteria
Spring Algal Group (Diatoms)	Summer Algal Group
Microzooplankton	Mesozooplankton
Dissolved Organic Carbon	Labile Particulate Organic Carbon
Refractory Particulate Organic Carbon	Ammonium
Nitrate	Dissolved Organic Nitrogen
Labile Particulate Organic Nitrogen	Refractory Particulate Organic Nitrogen
Total Phosphate	Dissolved Organic Phosphorus
Labile Particulate Organic Phosphorus	Refractory Particulate Organic Phosphorus
Chemical Oxygen Demand	Dissolved Oxygen
Particulate Biogenic Silica	Dissolved Silica

Table 2
Algal Production Parameters

Group	Parameter	Value	Units
Spring	Pmax	300	g C g^{-1} Chl day^{-1}
	Topt	20	°C
	KTg1	0.0025	$°C^{-2}$
	KTg2	0.012	$°C^{-2}$
	α	4.25	g C g^{-1} Chl E^{-1} m^{-2}
Summer	Pmax	300	g C g^{-1} Chl day^{-1}
	Topt	25	°C
	KTg1	0.0025	$°C^{-2}$
	KTg2	0.01	$°C^{-2}$
	α	4.25	g C g^{-1} Chl E^{-1} m^{-2}

Table 3
Algal Composition

Parameter	Regression	R^2	Model	Units
CChl	94	0.58	90 (spring) 75 (summer)	g C g^{-1} Chl
Anc	0.21	0.56	0.175	g N g^{-1} C
Apc	0.018	0.26	0.010	g P g^{-1} C
Asc	0.87	0.43	0.8 (spring) 0.3 (summer)	g Si g^{-1} C

Table 4
Reported Distributions of Carbon, Nitrogen, and Phosphorus

	Distribution	Reference
Carbon	Refractory fraction of algae averages 40% of ash-free dry weight	Foree and McCarty (1970)
	22% dissolved, 73% labile particulate, 5% refractory particulate	Pett (1989)
	33% dissolved, 33% labile particulate, 33% refractory particulate	Westrich and Berner (1984)
	7% dissolved, 63% labile particulate, 30% refractory particulate	Otsuki and Hanya (1972)
Nitrogen	5 to 7% dissolved inorganic, 30 to 50% dissolved organic, labile particulate > 22 to 44%, refractory particulate < 21 to 23%	Garber (1984)
	50% of particulate nitrogen is refractory	Grill and Richards (1964)
Phosphorus	6% dissolved organic, 64% labile particulate, 30% refractory particulate	Otsuki and Hanya (1972)
	24 to 27% dissolved inorganic, 42 to 56% dissolved organic, labile particulate > 4 to 16%, refractory particulate < 7 to 27%	Garber (1984)
	33% of particulate phosphorus is refractory	Grill and Richards (1964)

Table 5
Modeled Distribution of Algal Carbon, Nitrogen, Phosphorus, Silica

		Carbon	Nitrogen	Phosphorus	Silica
Mortality	Dissolved Inorganic	1.0	0.5	0.5	
	Dissolved Organic		0.3	0.5	
	Labile Particulate		0.15		1.0
	Refractory Particulate		0.05		
Predation	Dissolved Inorganic		0.5	0.5	0.5
	Dissolved Organic	0.25	0.3	0.4	
	Labile Particulate	0.5	0.15	0.07	0.5
	Refractory Particulate	0.25	0.05	0.03	

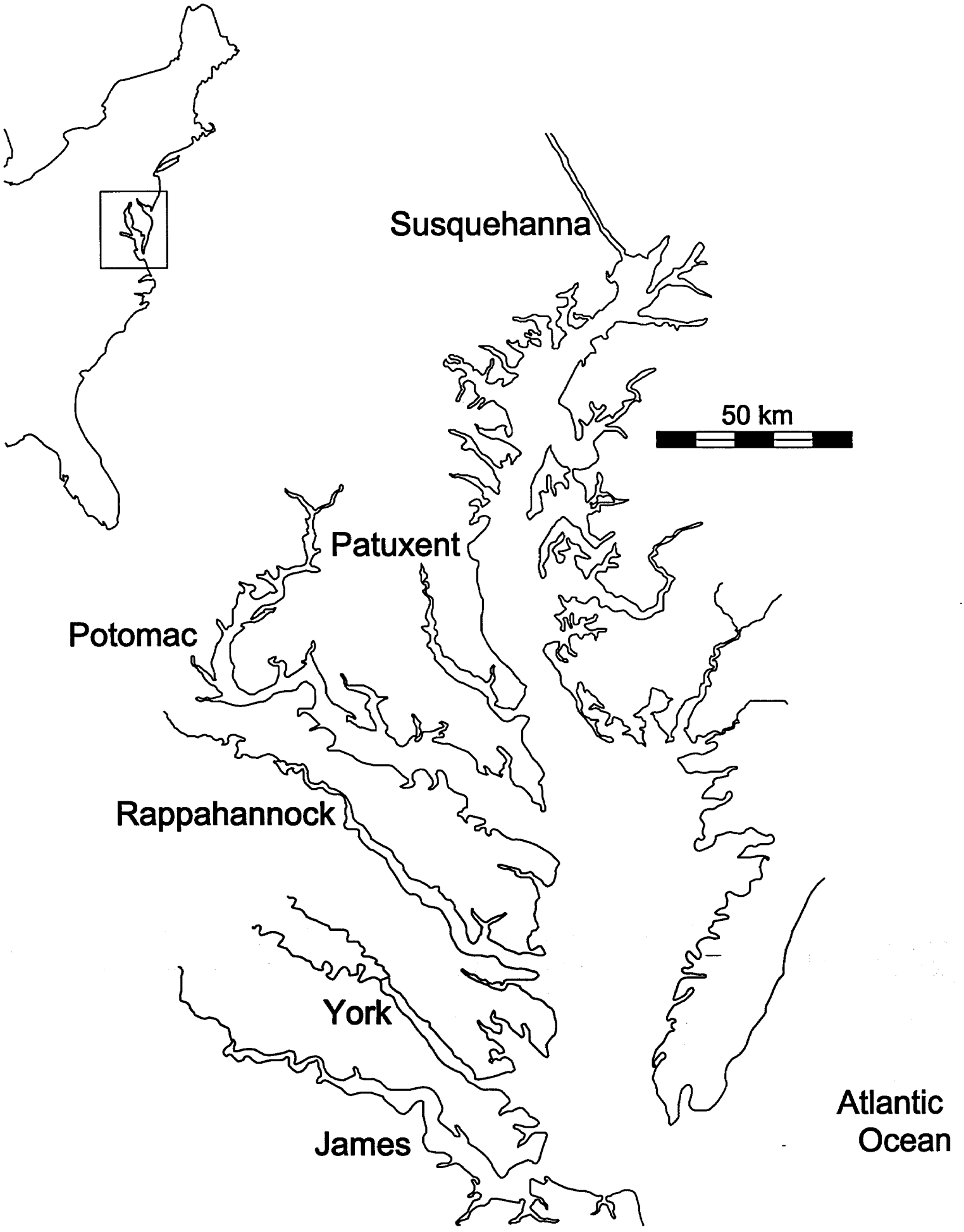
Susquehanna
50 km
Patuxent
Potomac
Rappahannock
York
James
Atlantic
Ocean

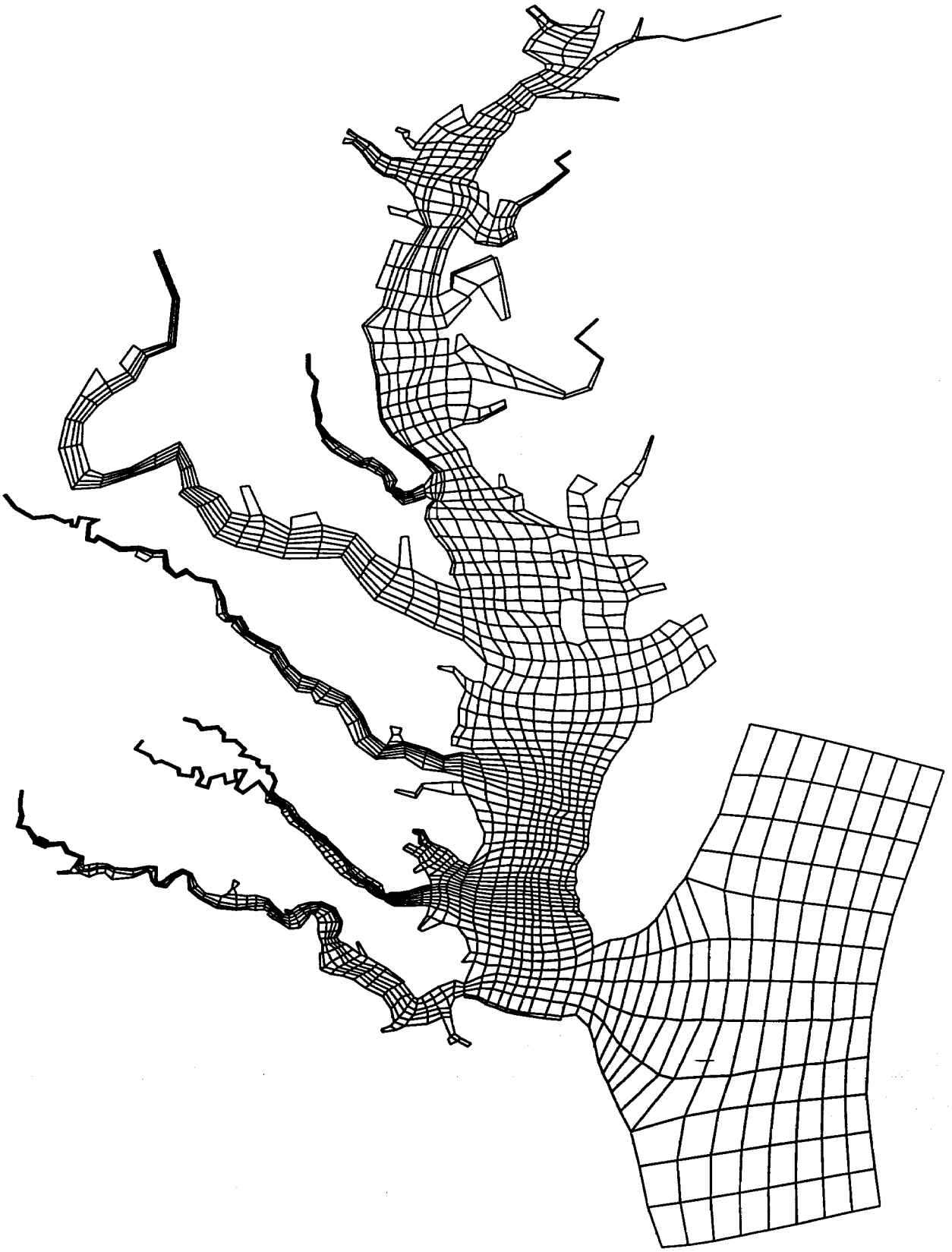

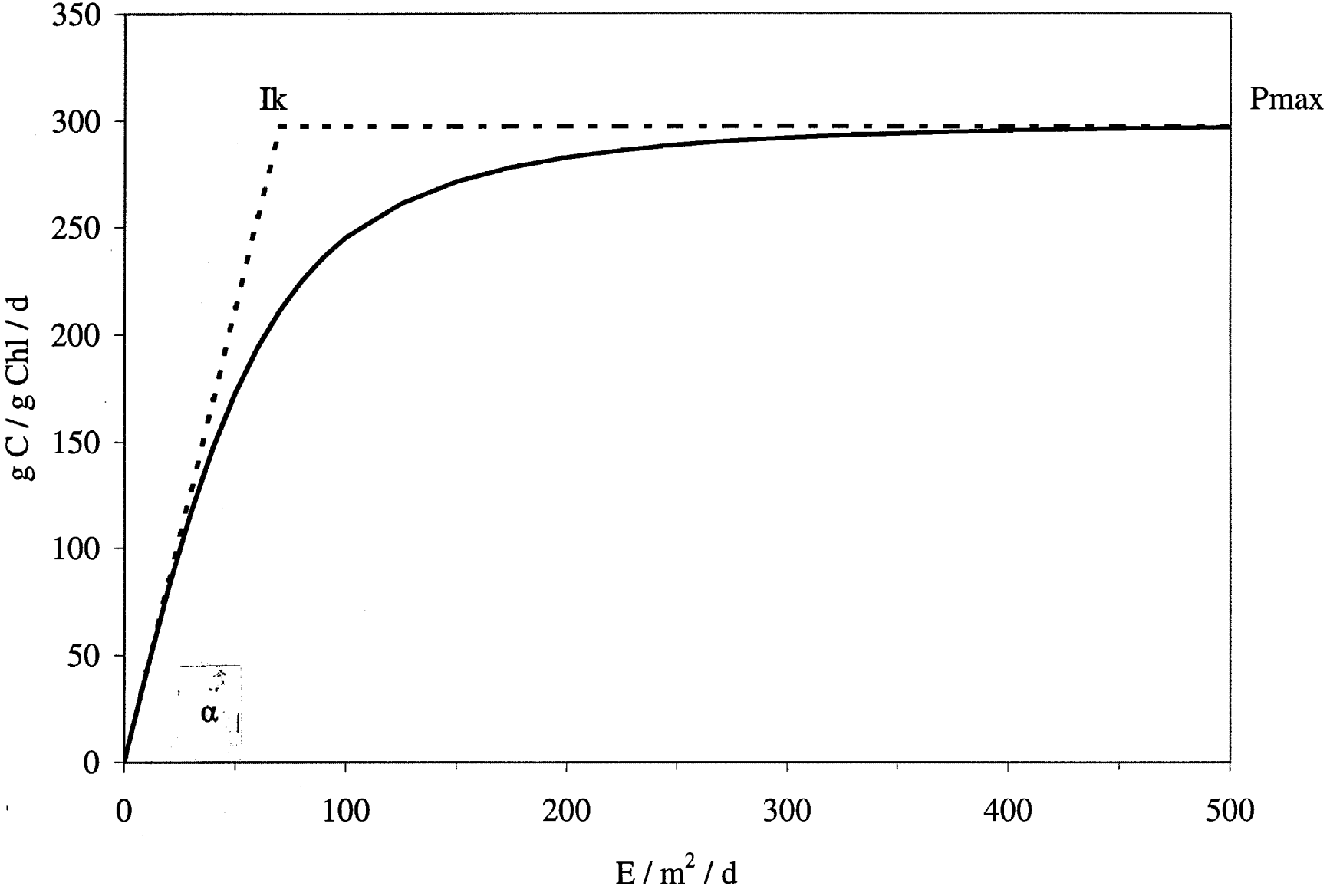
350
300
250
200
150
100
50
0
Ik
Pmax
α
g C / g Chl / d
0
100
200
300
400
500
E / m2 / d

Figure 2

FIGURE 4

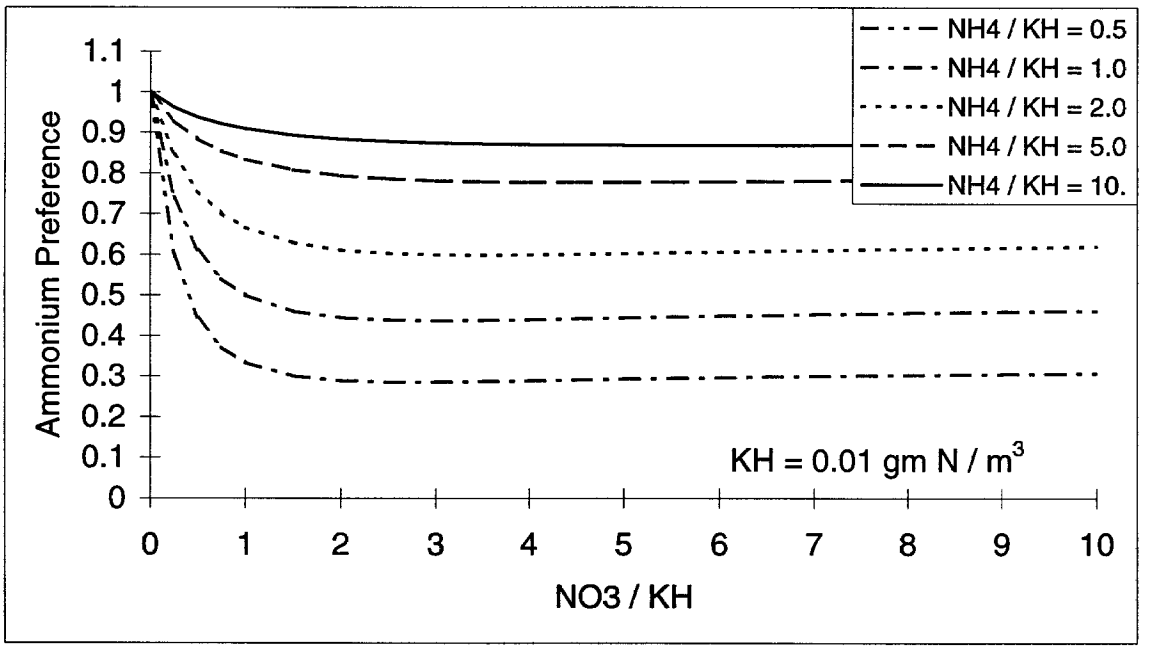

D:\bagrpt\kinplots

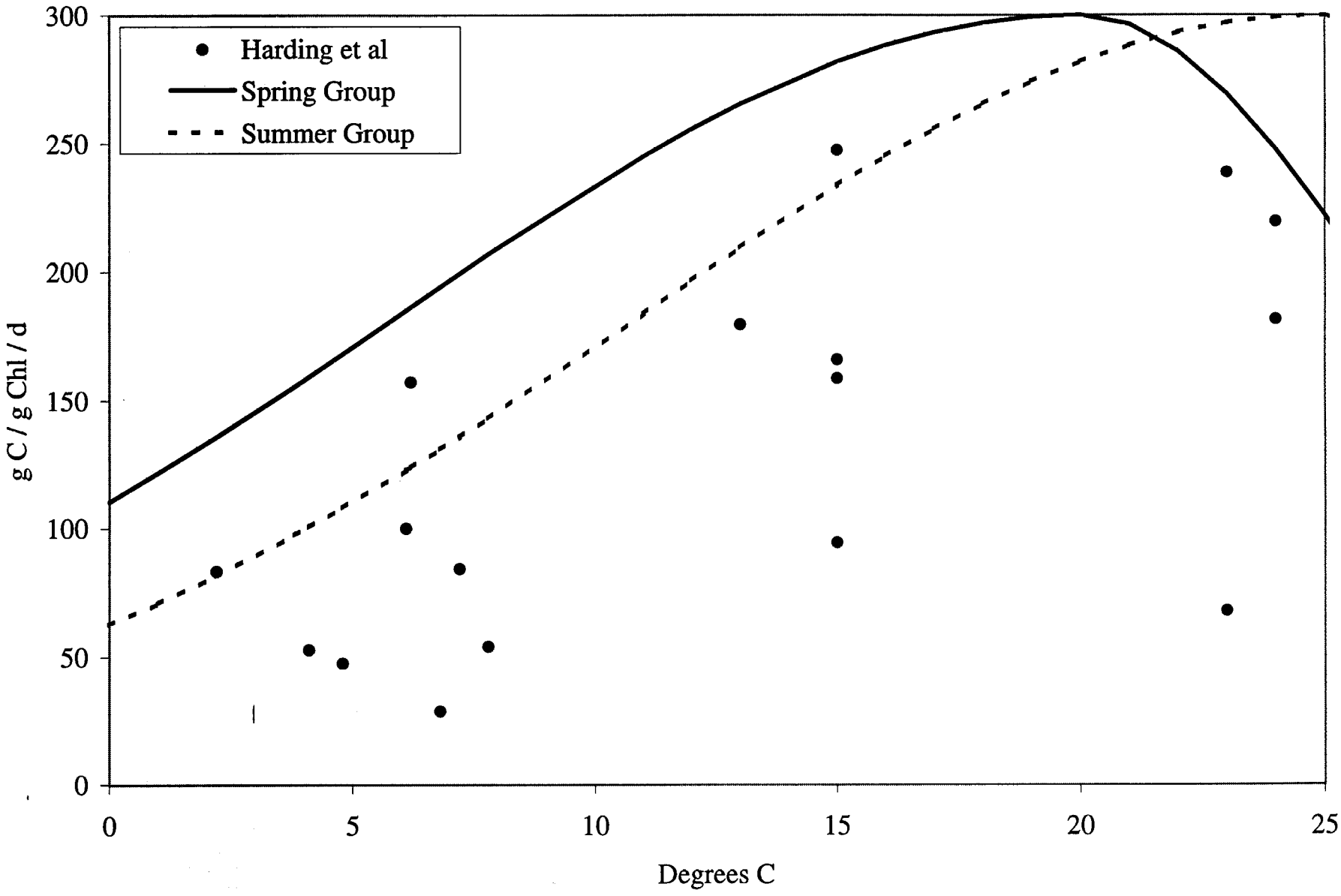
Harding et al
Spring Group
Summer Group
300
250
200
150
100
50
0
g C / g Chl / d
0
5
10
15
20
25
Degrees C

Figure 5

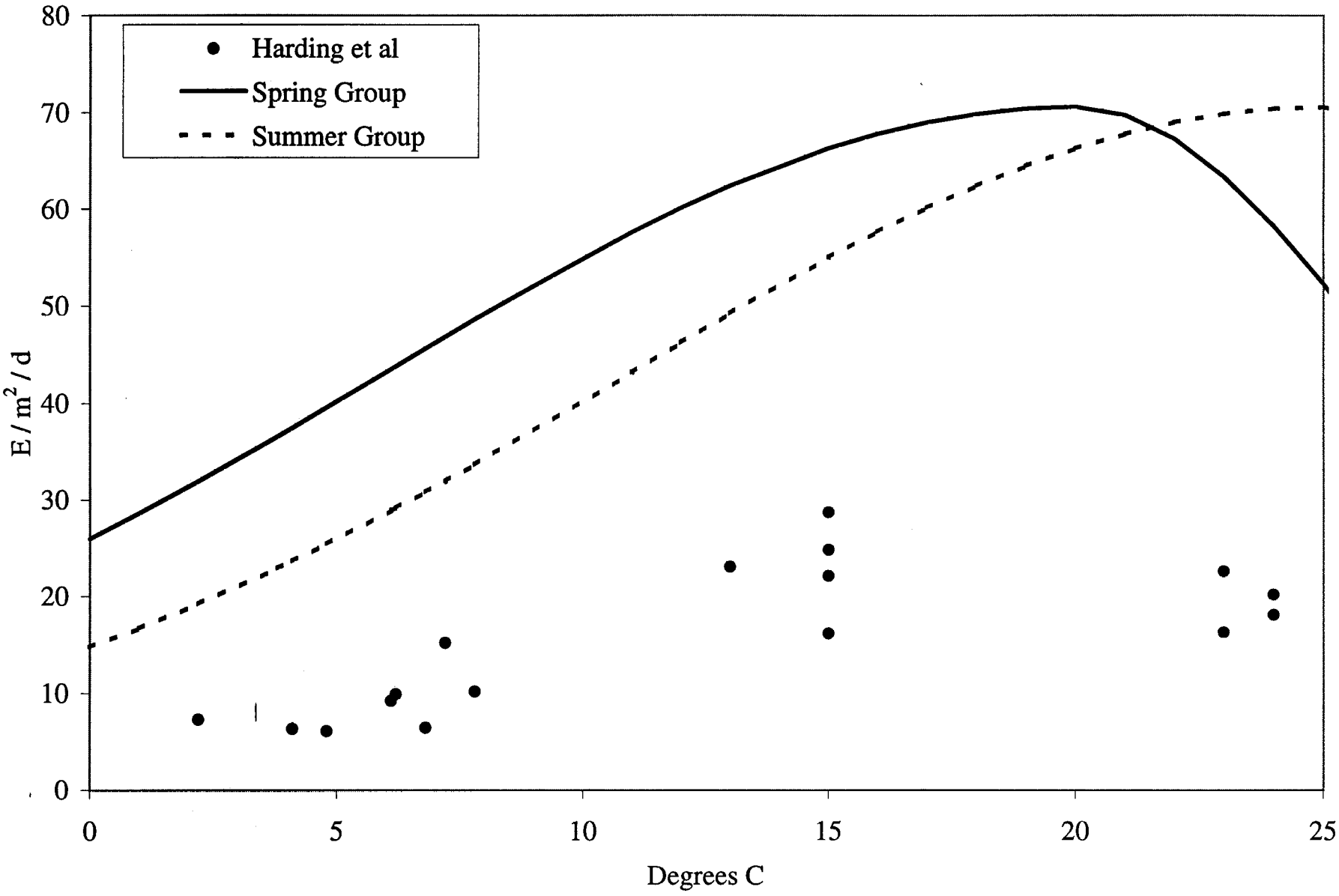
Harding et al
Spring Group
Summer Group
E / m² / d
Degrees C
0
10
20
30
40
50
60
70
80
0
5
10
15
20
25

FIGURE 6

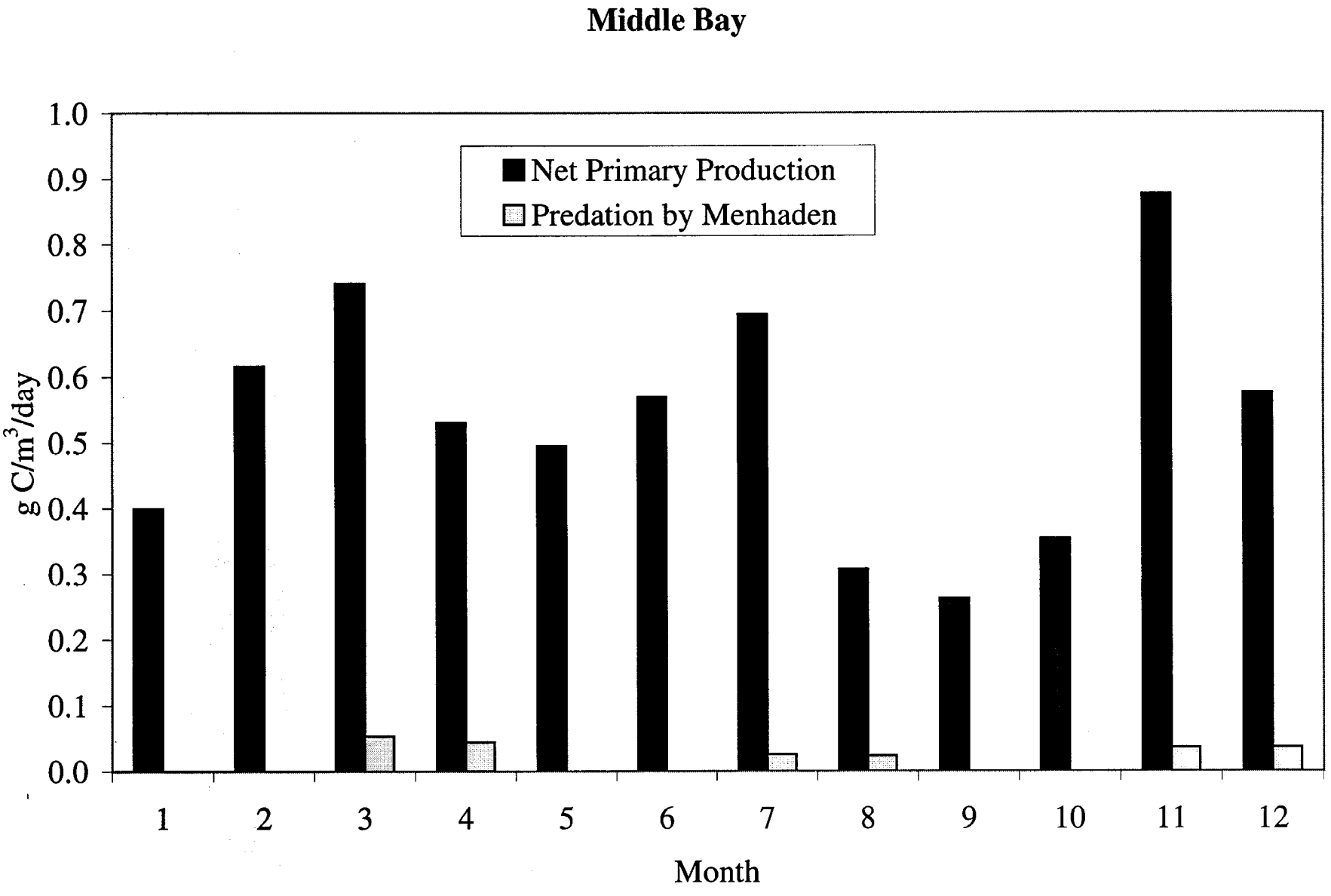
Middle Bay
Net Primary Production
Predation by Menhaden
g C/m3/day
1.0
0.9
0.8
0.7
0.6
0.5
0.4
0.3
0.2
0.1
0.0
1
2
3
4
5
6
7
8
9
10
11
12
Month

Figure 7

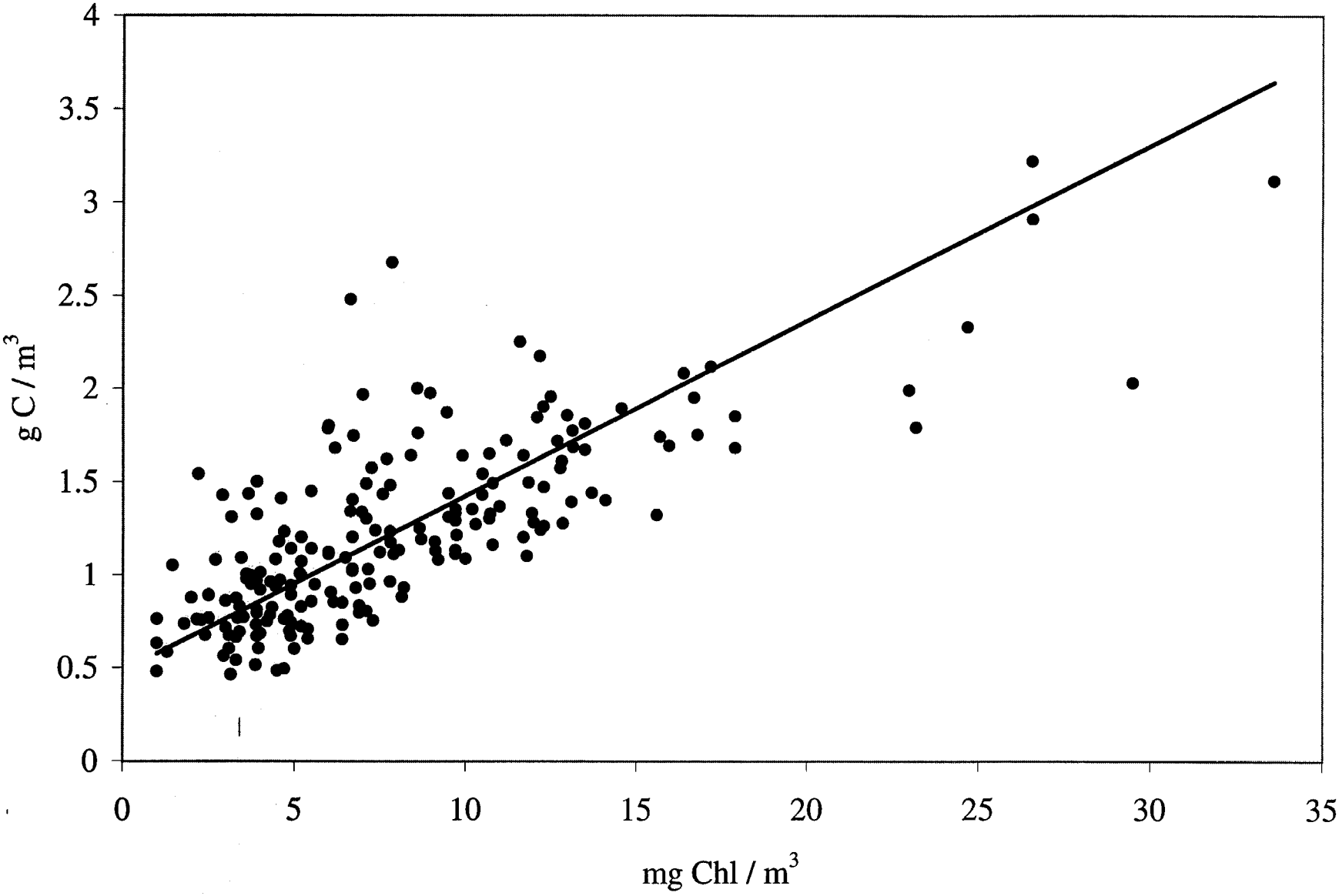

Figure 8

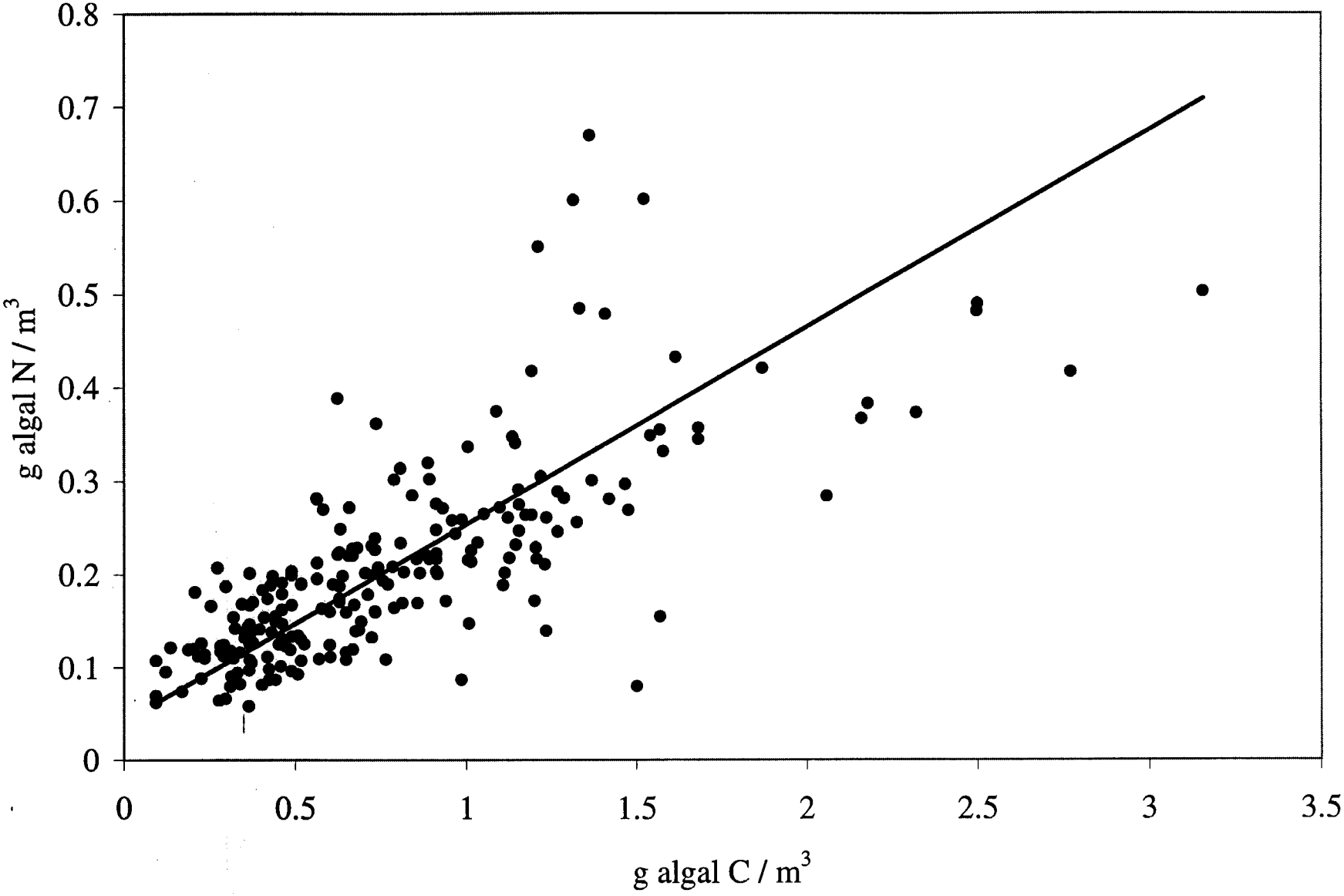

Figure 9

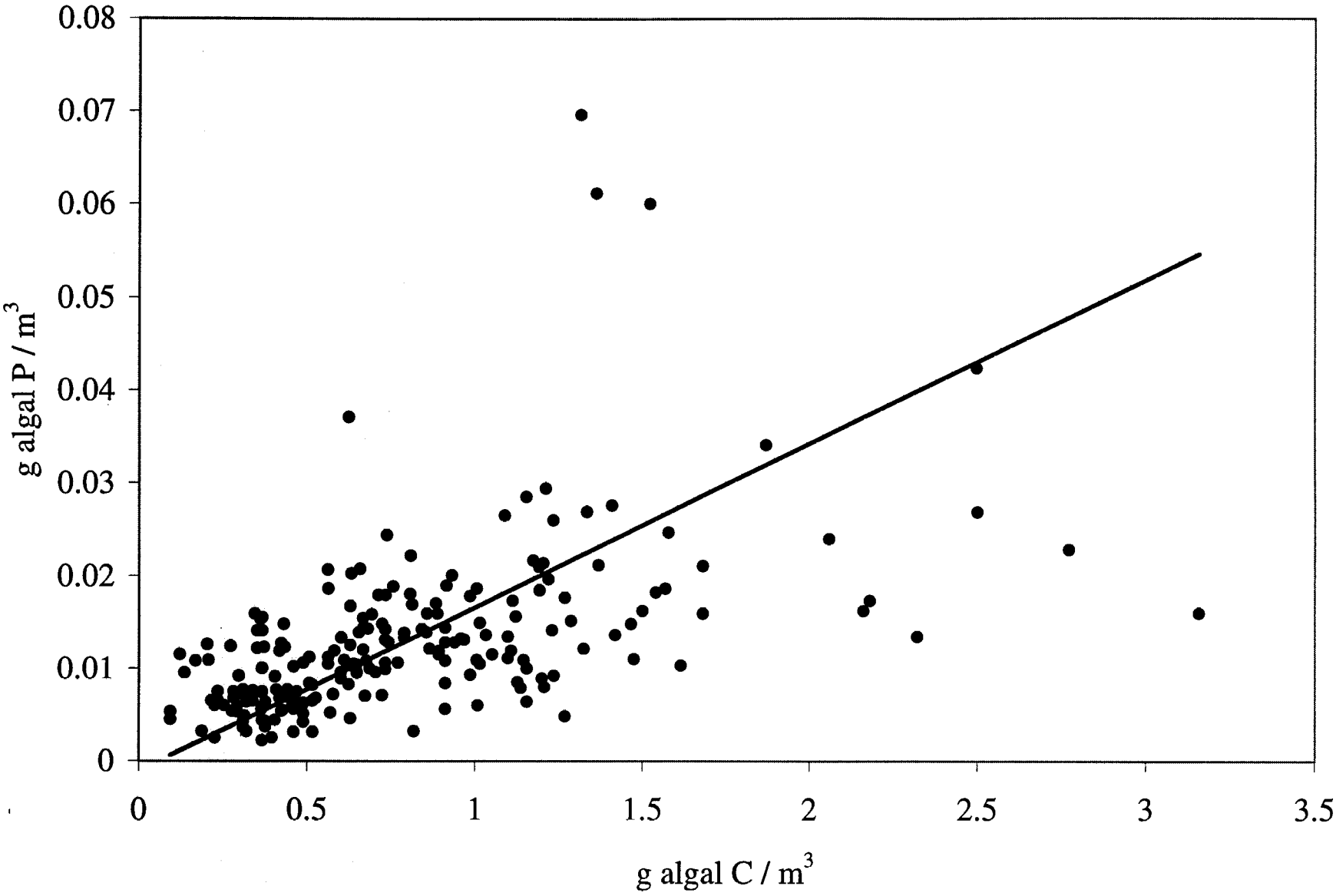
0.08
0.07
0.06
0.05
0.04
0.03
0.02
0.01
0
g algal P / m3
0
0.5
1
1.5
2
2.5
3
3.5
g algal C / m3

Figure 10

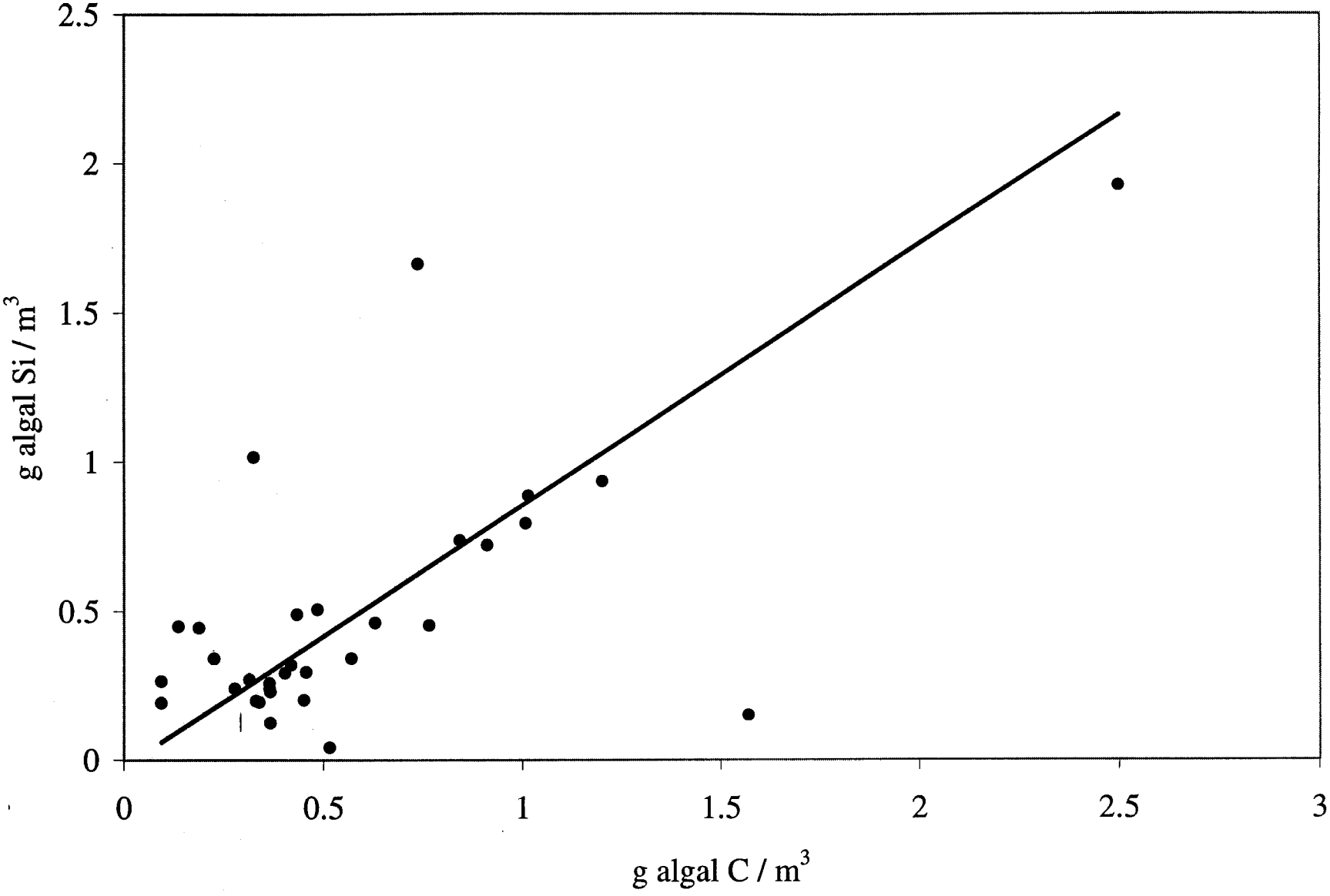
2.5
2
1.5
1
0.5
0
0
0.5
1
1.5
2
2.5
3
g algal Si / m3
g algal C / m3

Figure 12

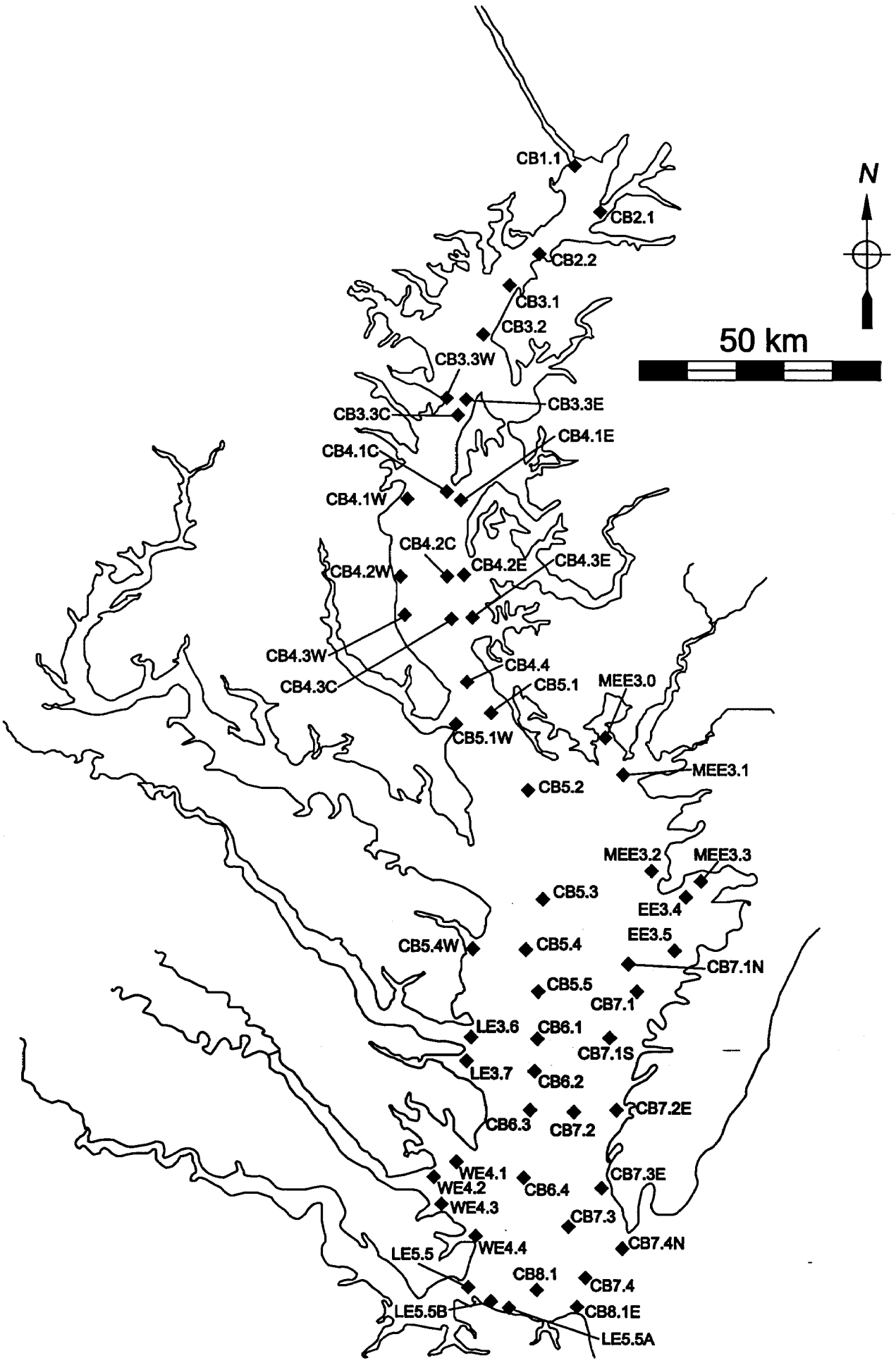
CB1.1
CB2.1
CB2.2
CB3.1
CB3.2
CB3.3W
CB3.3E
CB3.3C
CB4.1E
CB4.1C
CB4.1W
CB4.2C
CB4.2E
CB4.3E
CB4.2W
CB4.3W
CB4.3C
CB4.4
CB5.1
MEE3.0
CB5.1W
MEE3.1
CB5.2
MEE3.2
MEE3.3
CB5.3
EE3.4
EE3.5
CB5.4W
CB5.4
CB7.1N
CB5.5
CB7.1
LE3.6
CB6.1
CB7.1S
LE3.7
CB6.2
CB7.2E
CB6.3
CB7.2
WE4.1
CB7.3E
WE4.2
CB6.4
WE4.3
CB7.3
WE4.4
CB7.4N
LE5.5
CB8.1
CB7.4
LE5.5B
CB8.1E
LE5.5A
N
50 km

MAINSTEM BAY, RUN 169NEW (Spring 1989–92) 7/30/99

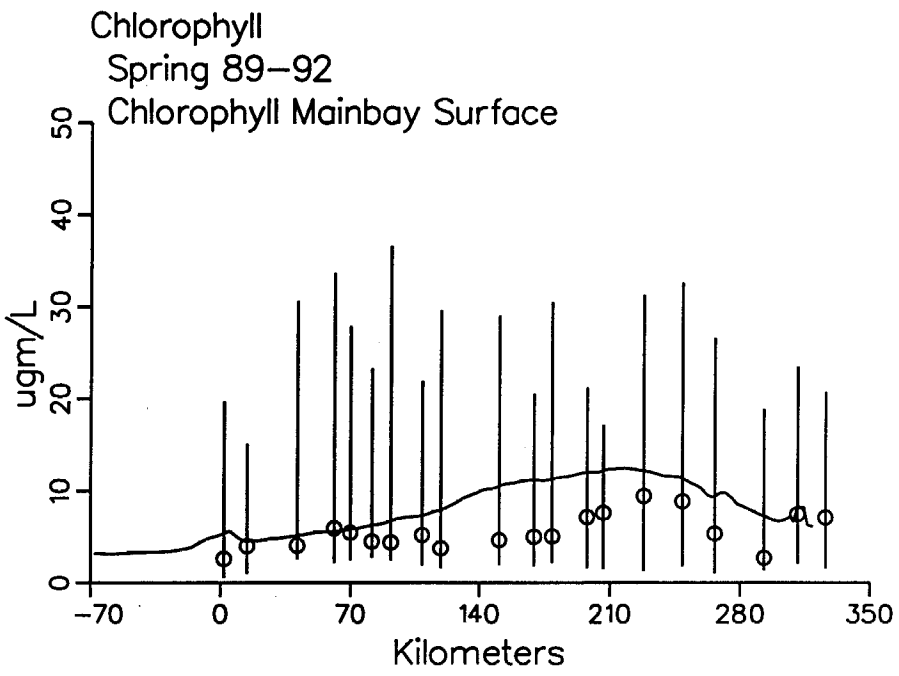

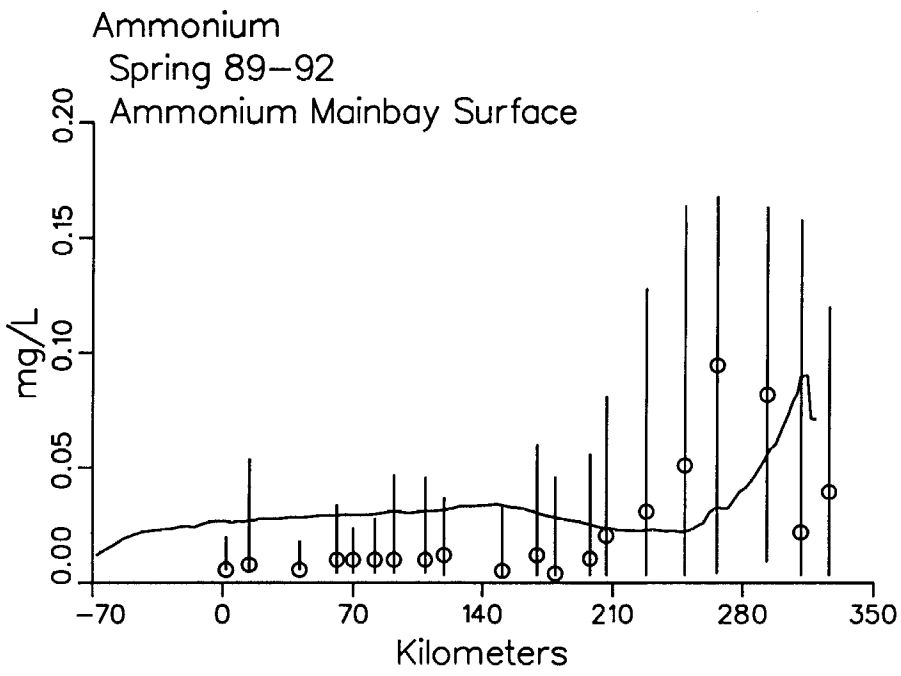

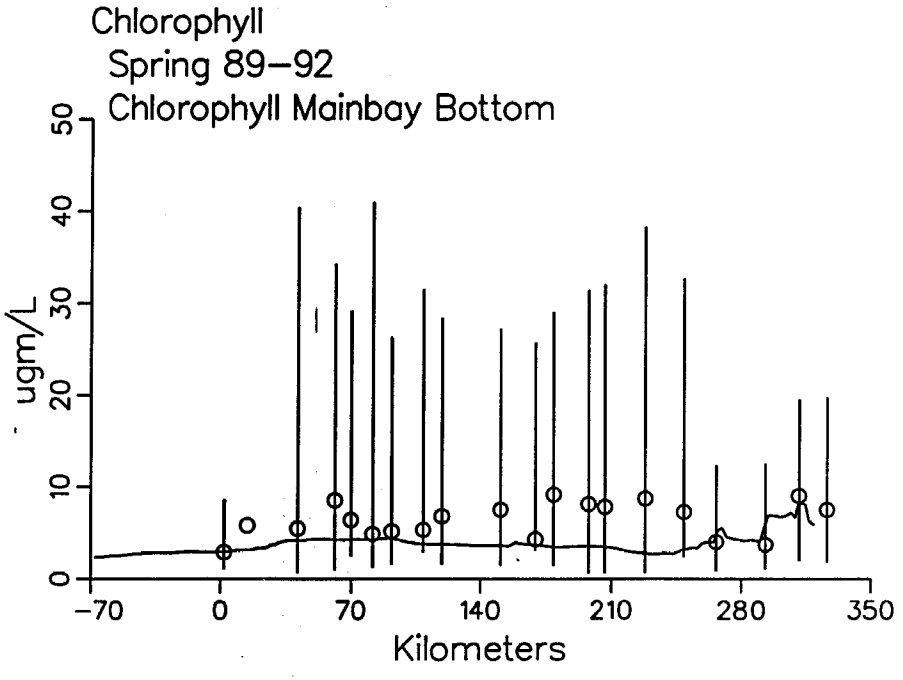

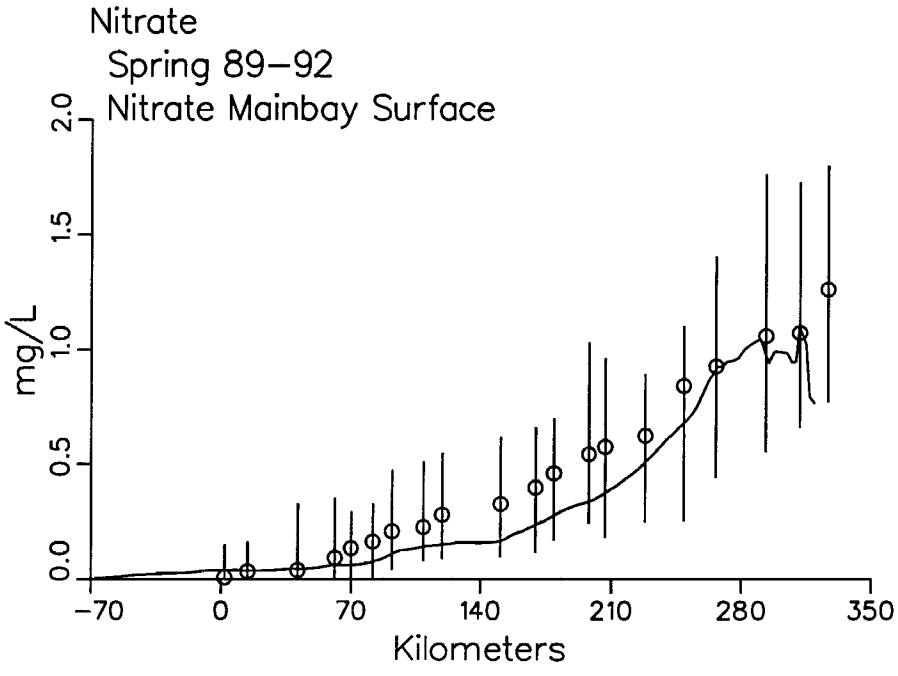

Figure 13 1/2

Dissolved Inorganic Phosphorus
Spring 89–92
PO4 Mainbay Surface

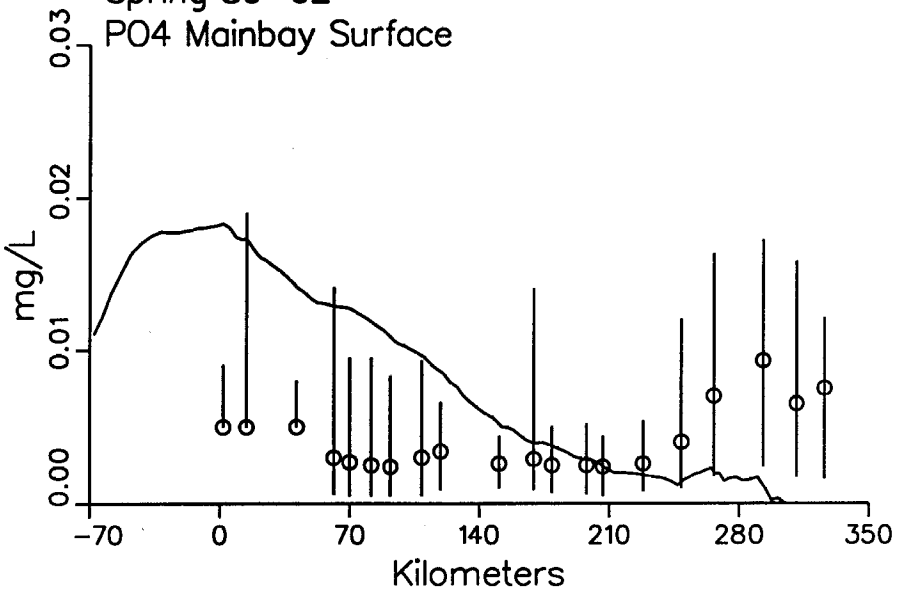

Light Extinction
Spring 89–92
Light Extinction Mainbay Surface

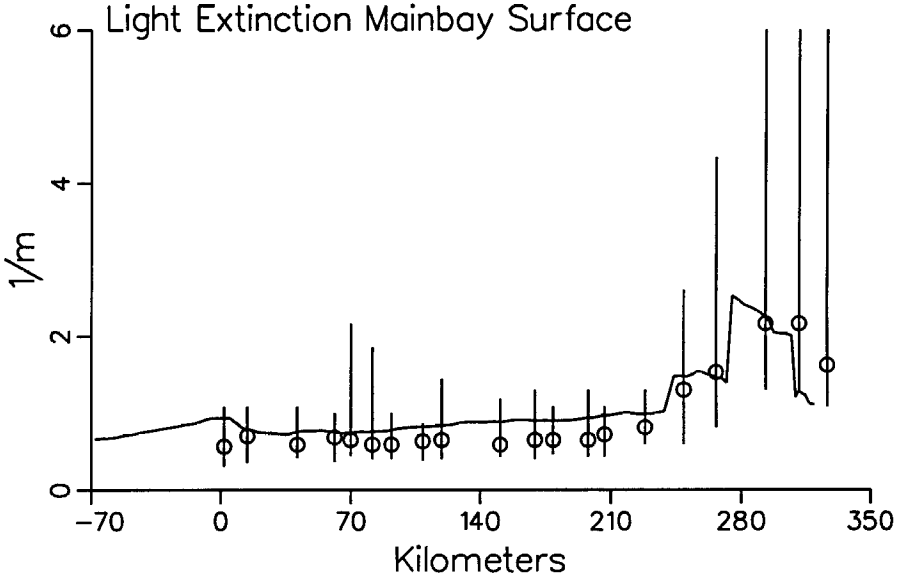

Dissolved Silica
Spring 89–92
Dis. Silica Mainbay Surface

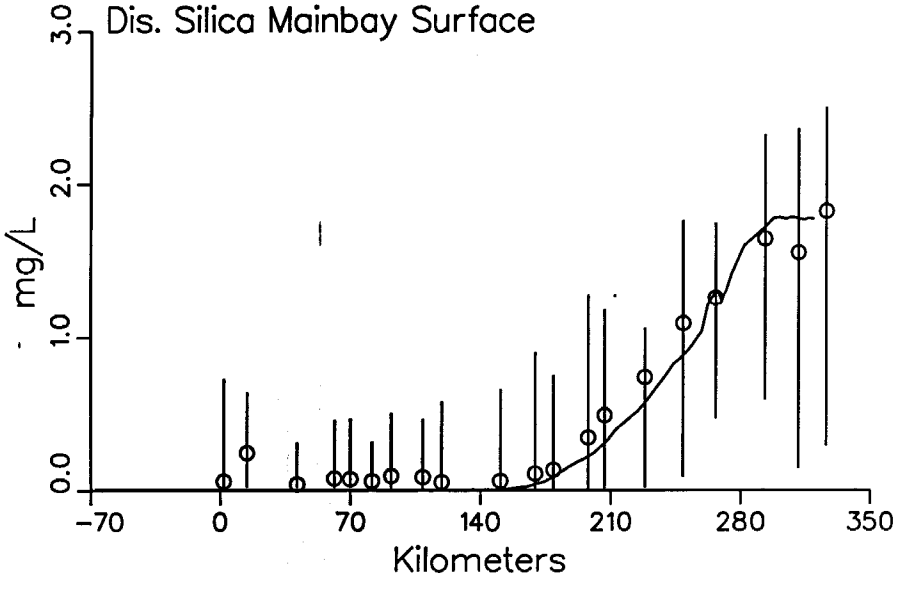

FIGURE 13 2/2

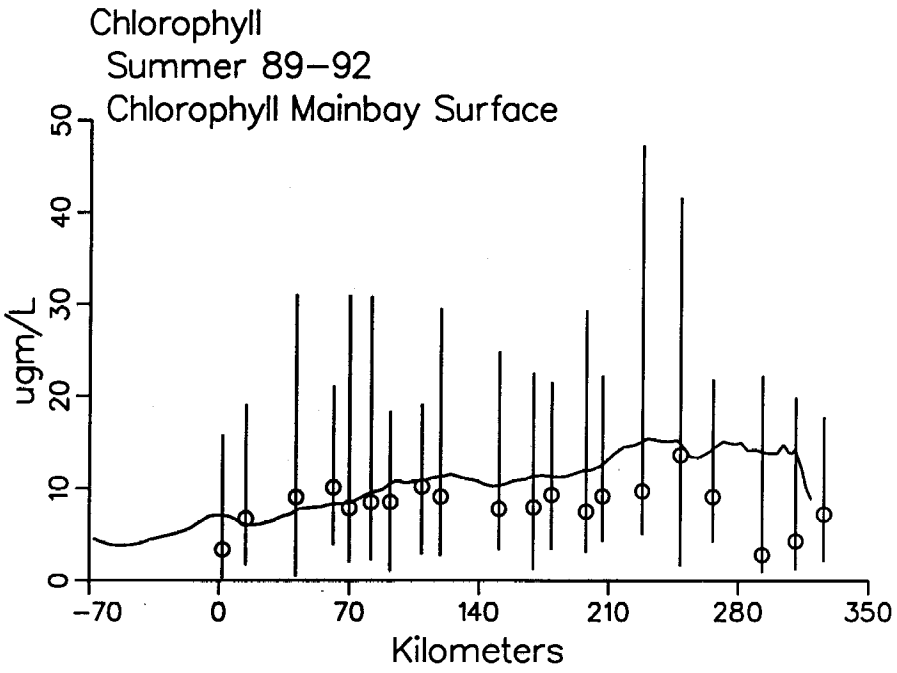
Chlorophyll
Summer 89–92
Chlorophyll Mainbay Surface
ugm/L
0
10
20
30
40
50
–70
0
70
140
210
280
350
Kilometers

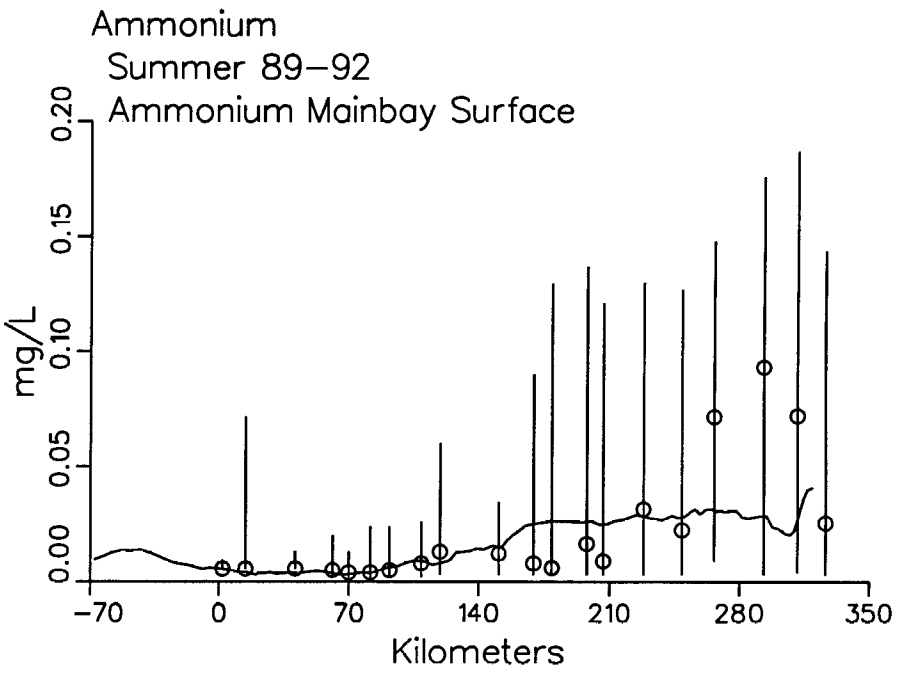
Ammonium
Summer 89–92
Ammonium Mainbay Surface
mg/L
0.00
0.05
0.10
0.15
0.20
–70
0
70
140
210
280
350
Kilometers

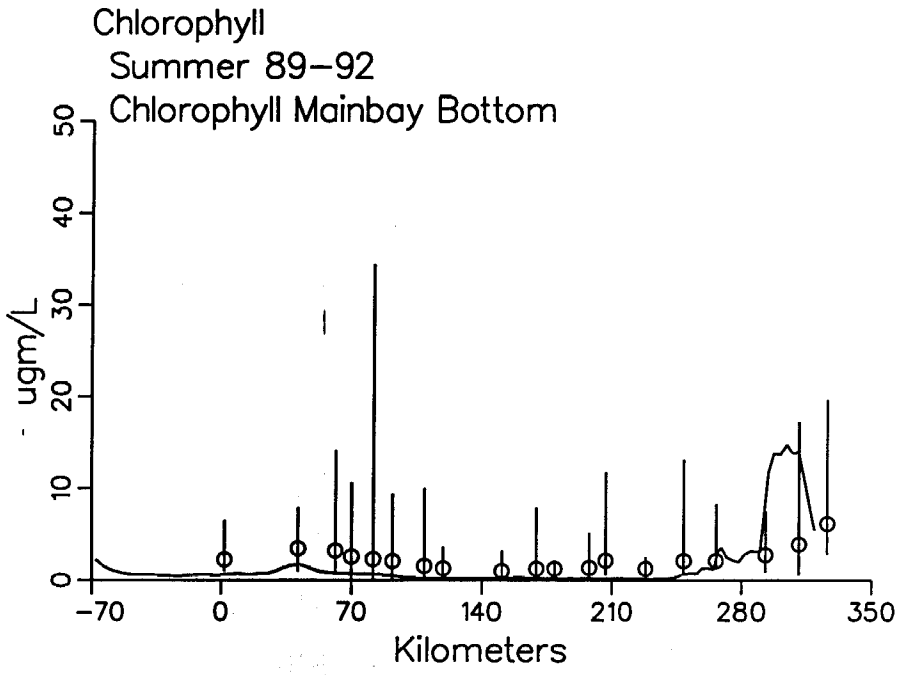
Chlorophyll
Summer 89–92
Chlorophyll Mainbay Bottom
ugm/L
0
10
20
30
40
50
–70
0
70
140
210
280
350
Kilometers

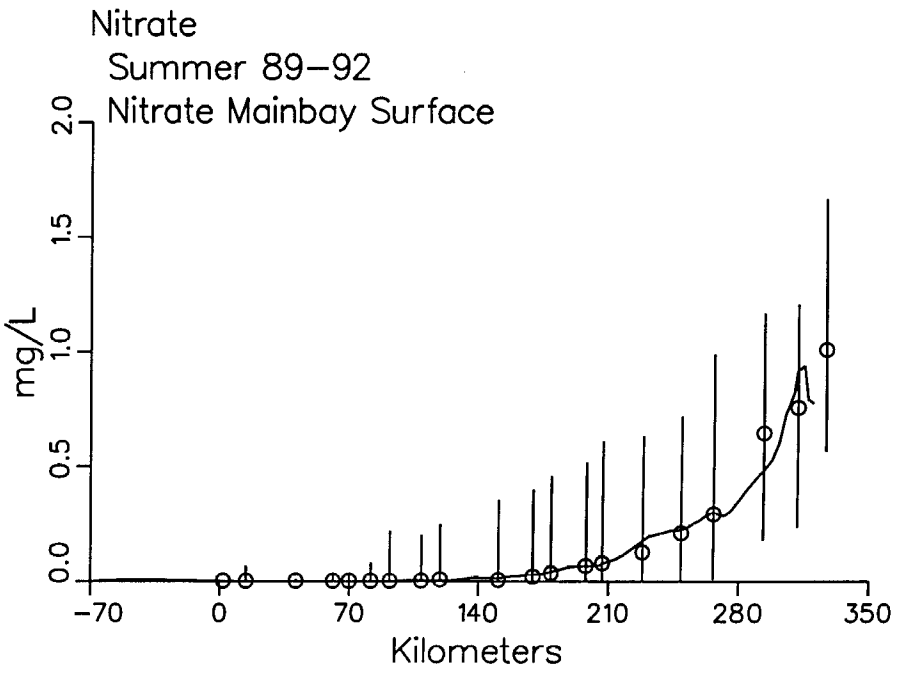
Nitrate
Summer 89–92
Nitrate Mainbay Surface
mg/L
0.0
0.5
1.0
1.5
2.0
–70
0
70
140
210
280
350
Kilometers

MAINSTEM BAY, RUN 169NEW (Summer 1989–92) 7/30/99

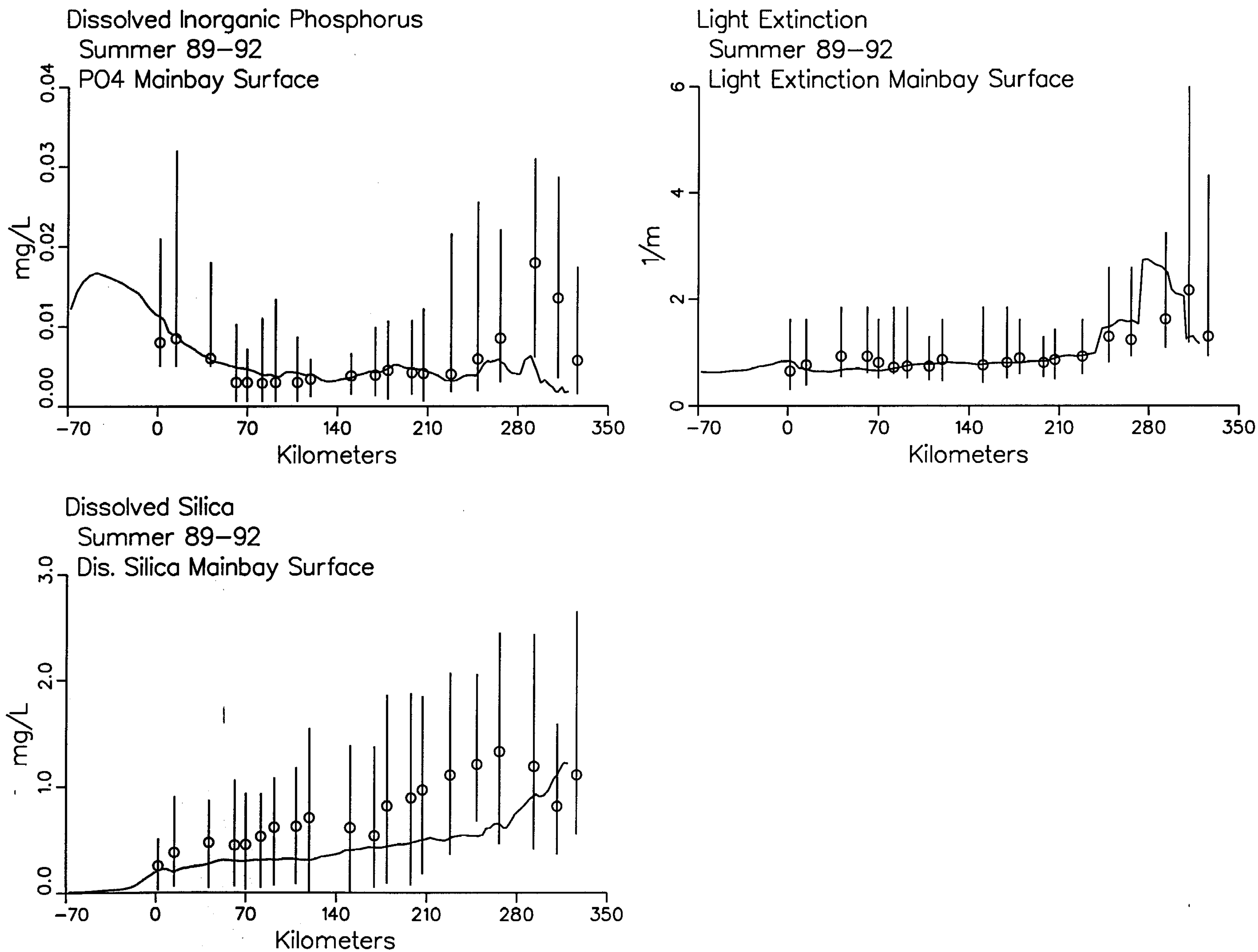

FIGURE 14 2/2

RUN 169NEW MAJOR CBPS CELL 741 AND STATION CB5.2 DATA 7/30/99

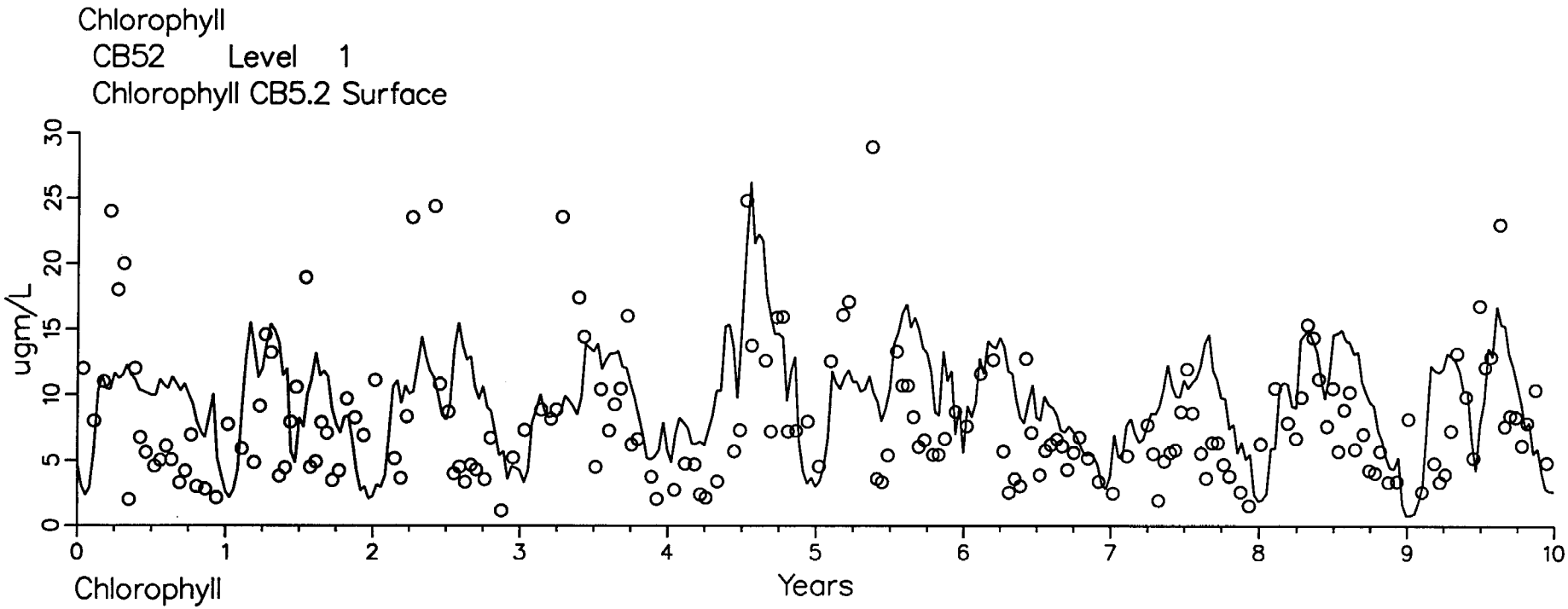

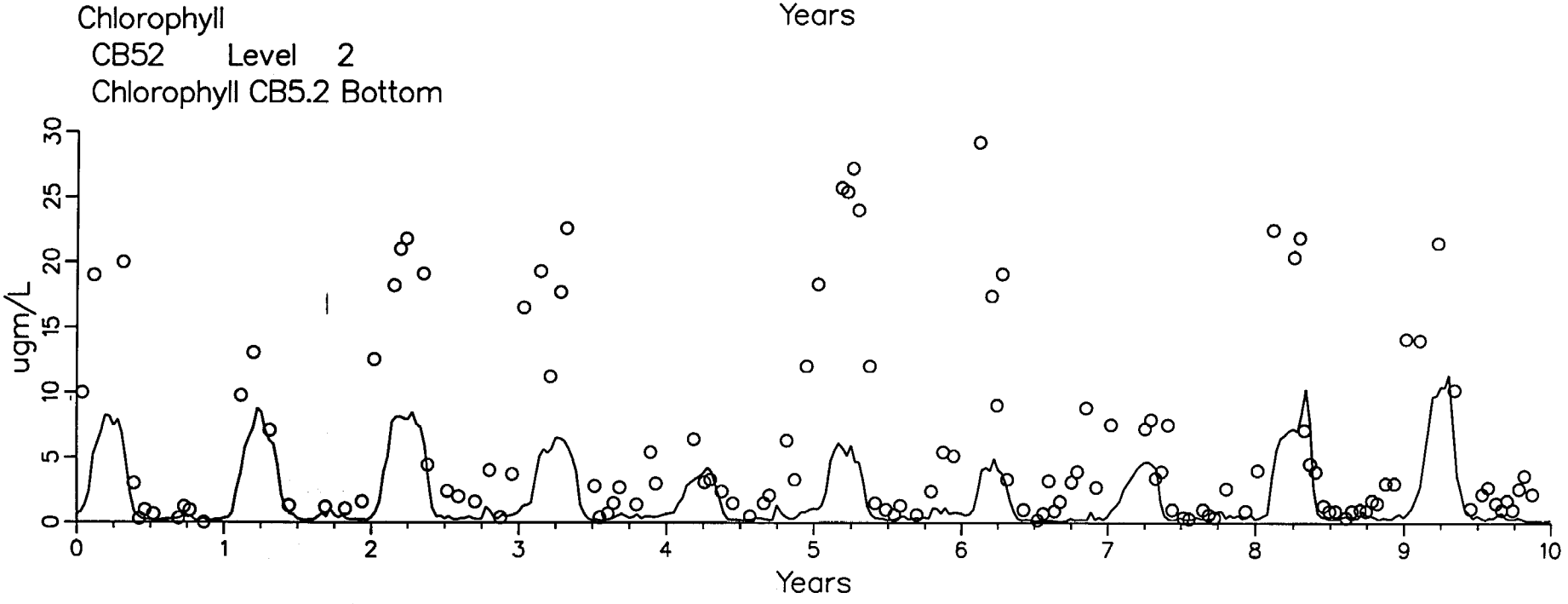

FIGURE 15 1/4

RUN 169NEW MAJOR CBPS CELL 741 AND STATION CB5.2 DATA 7/30/99

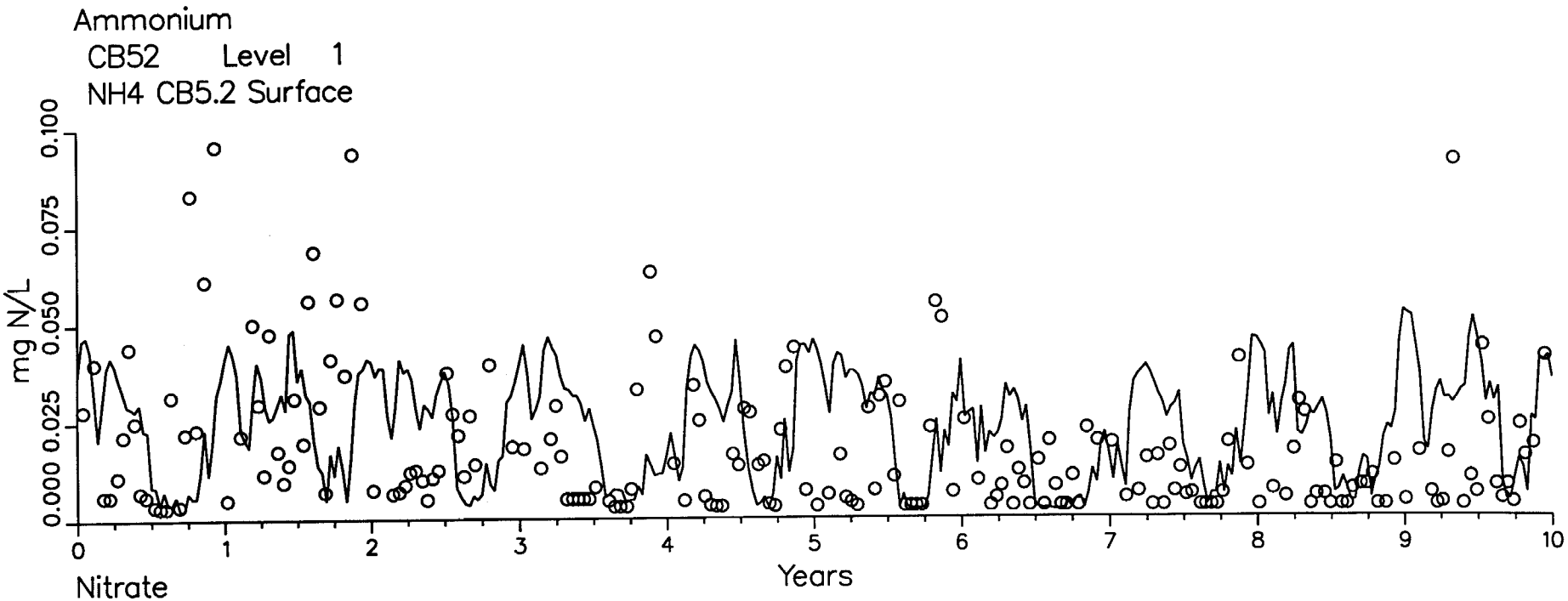

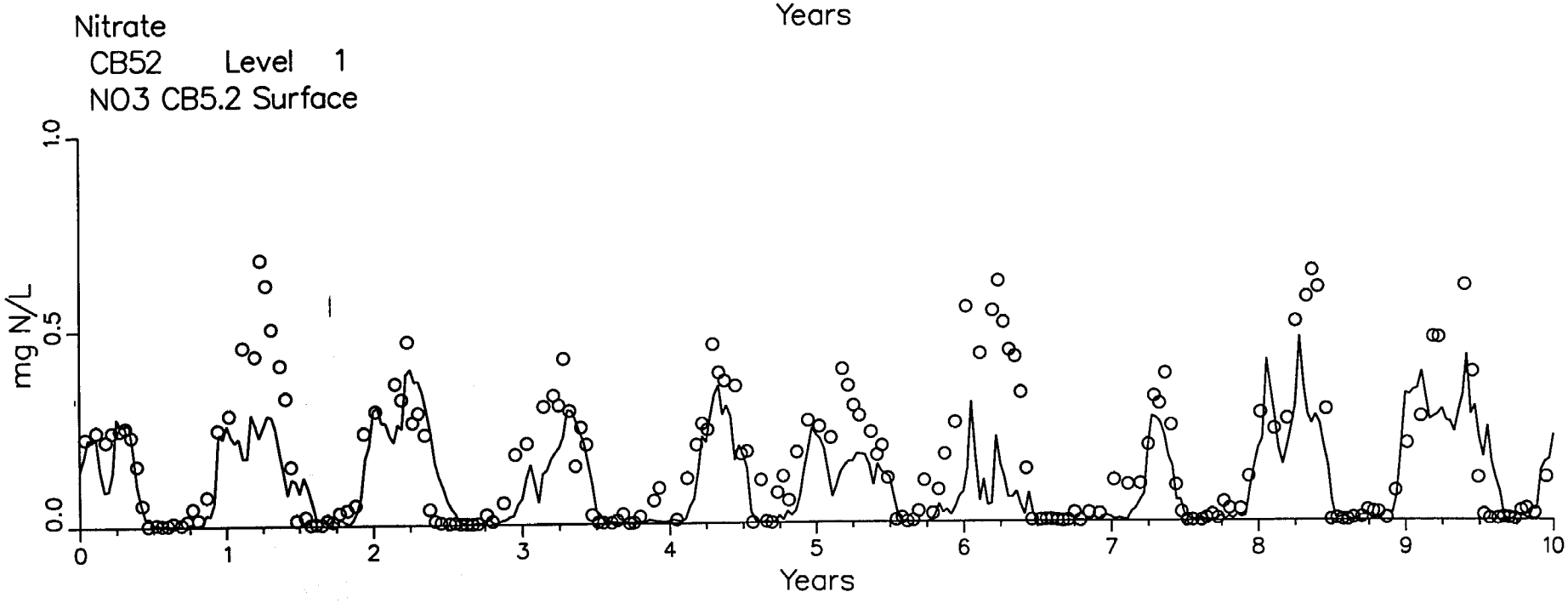

Figure 15 of 24

RUN 169NEW MAJOR CBPS CELL 741 AND STATION CB5.2 DATA 7/30/99

Dissolved Inorganic Phosphorus
CB52 Level 1
P04 CB5.2 Surface

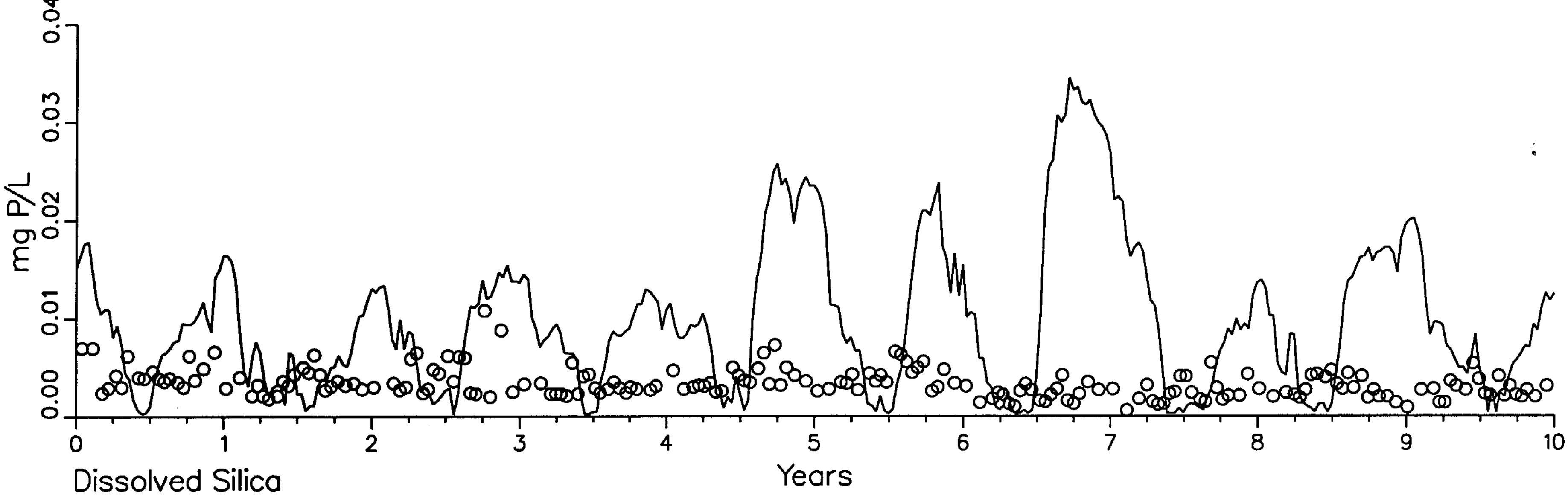

Dissolved Silica
CB52 Level 1
Dis. Silica CB5.2 Surface

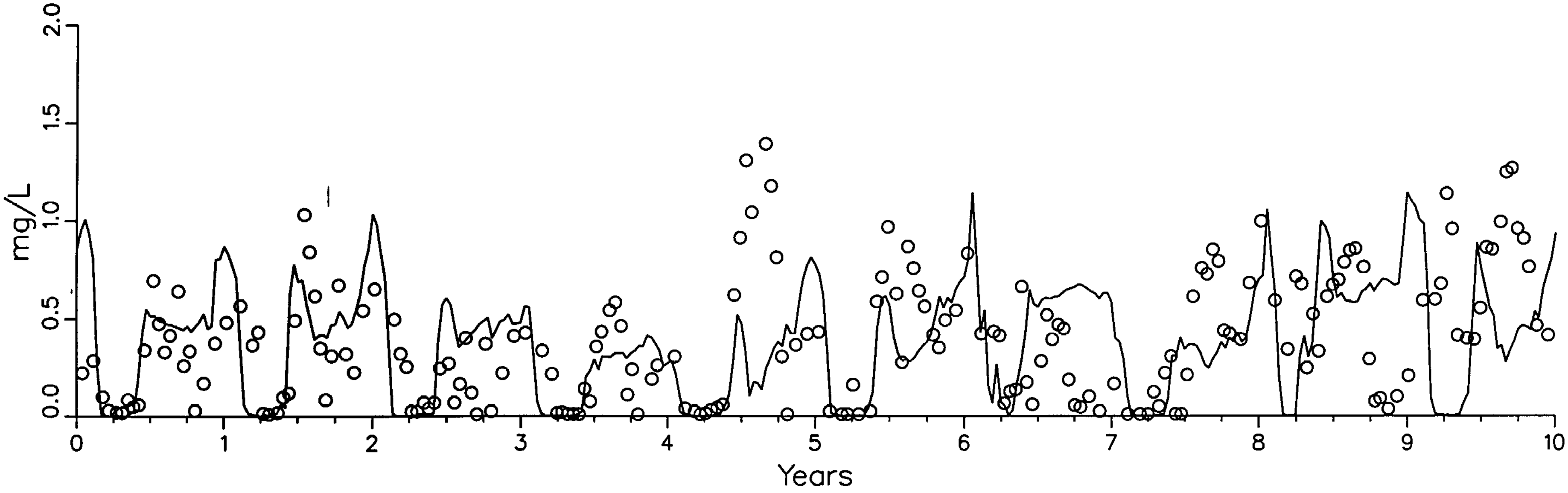

Figure 15b 3/4

RUN 169NEW MAJOR CBPS CELL 741 AND STATION CB5.2 DATA 7/30/99

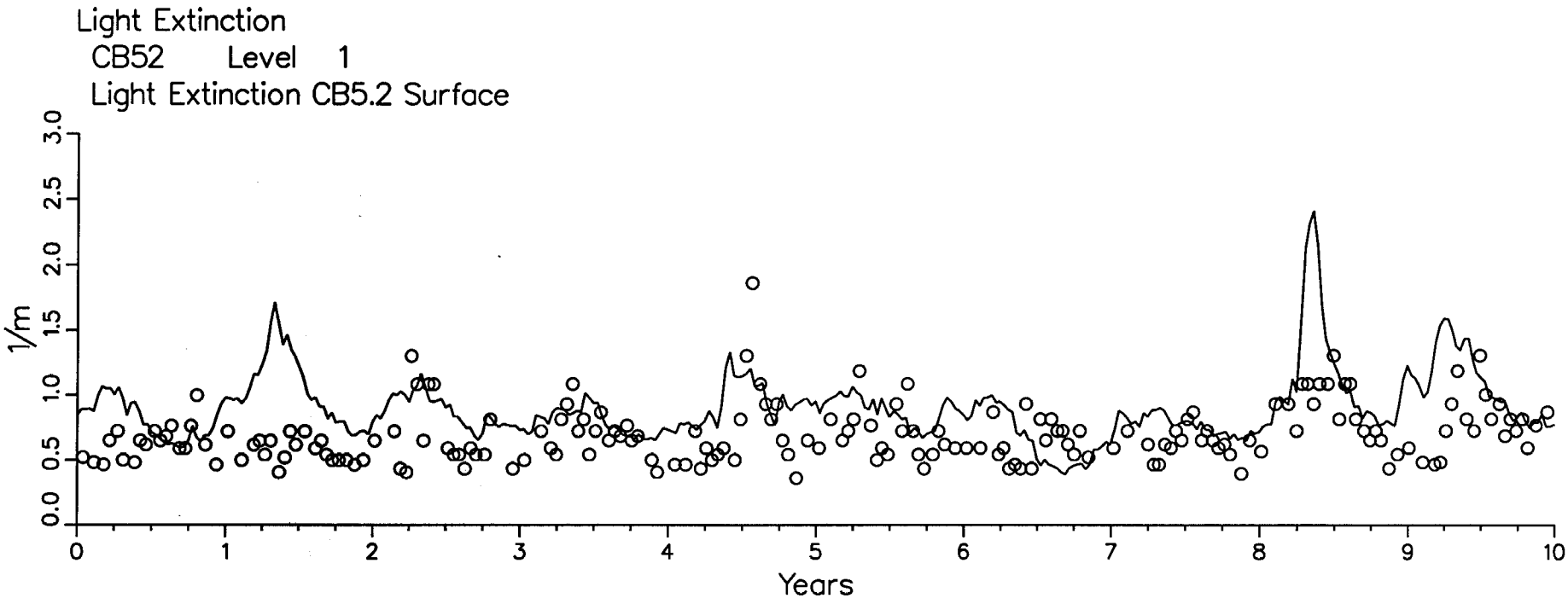

Figure 15 #1/4

Growth Limits at Station CB2.2

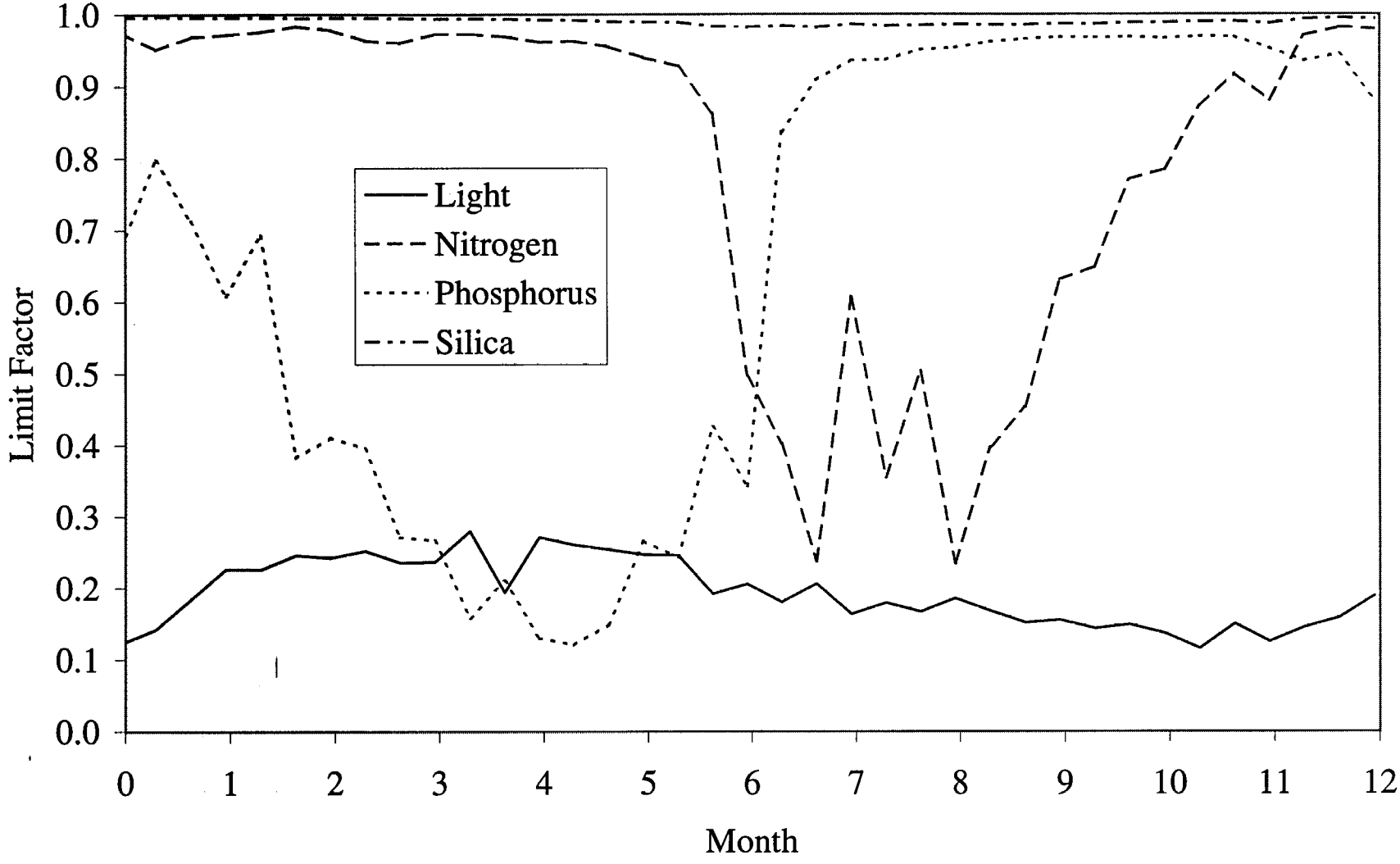

Figure 16

FIGURE 17

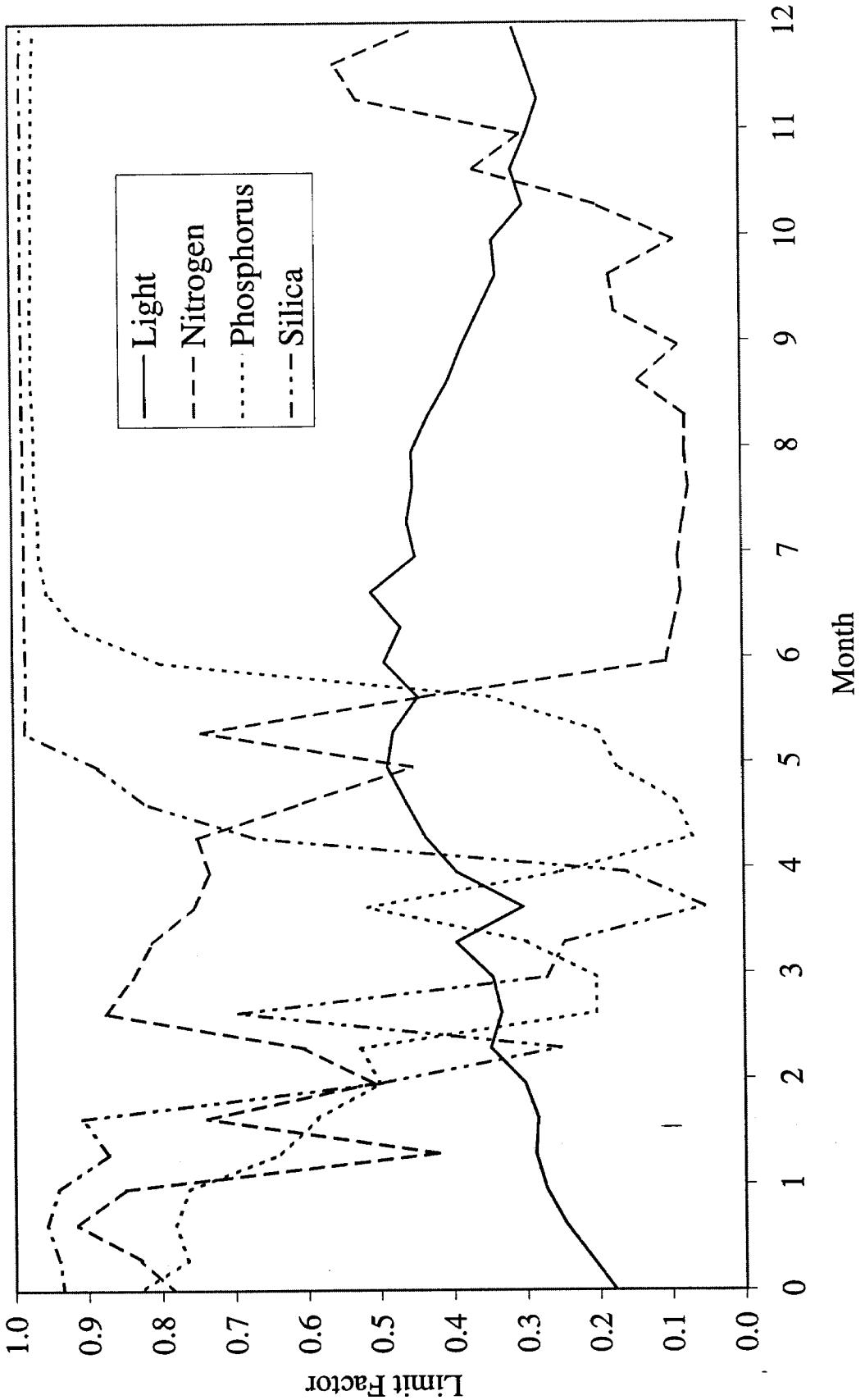
Growth Limits at Station CB5.2
Light
Nitrogen
Phosphorus
Silica
Limit Factor
1.0
0.9
0.8
0.7
0.6
0.5
0.4
0.3
0.2
0.1
0.0
0
1
2
3
4
5
6
7
8
9
10
11
12
Month

Growth Limits at Station CB7.3

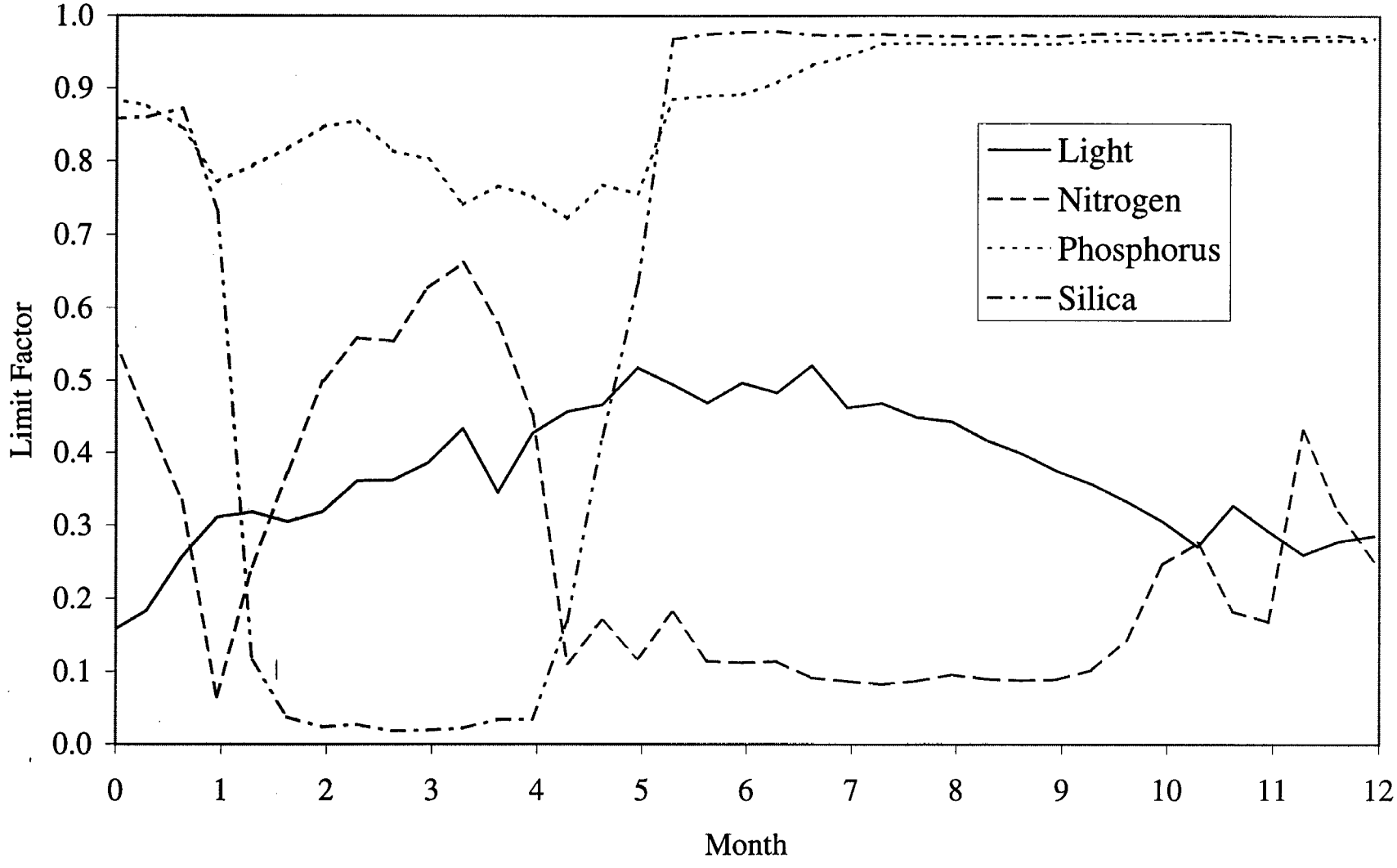

Figure 18

FIGURE 19

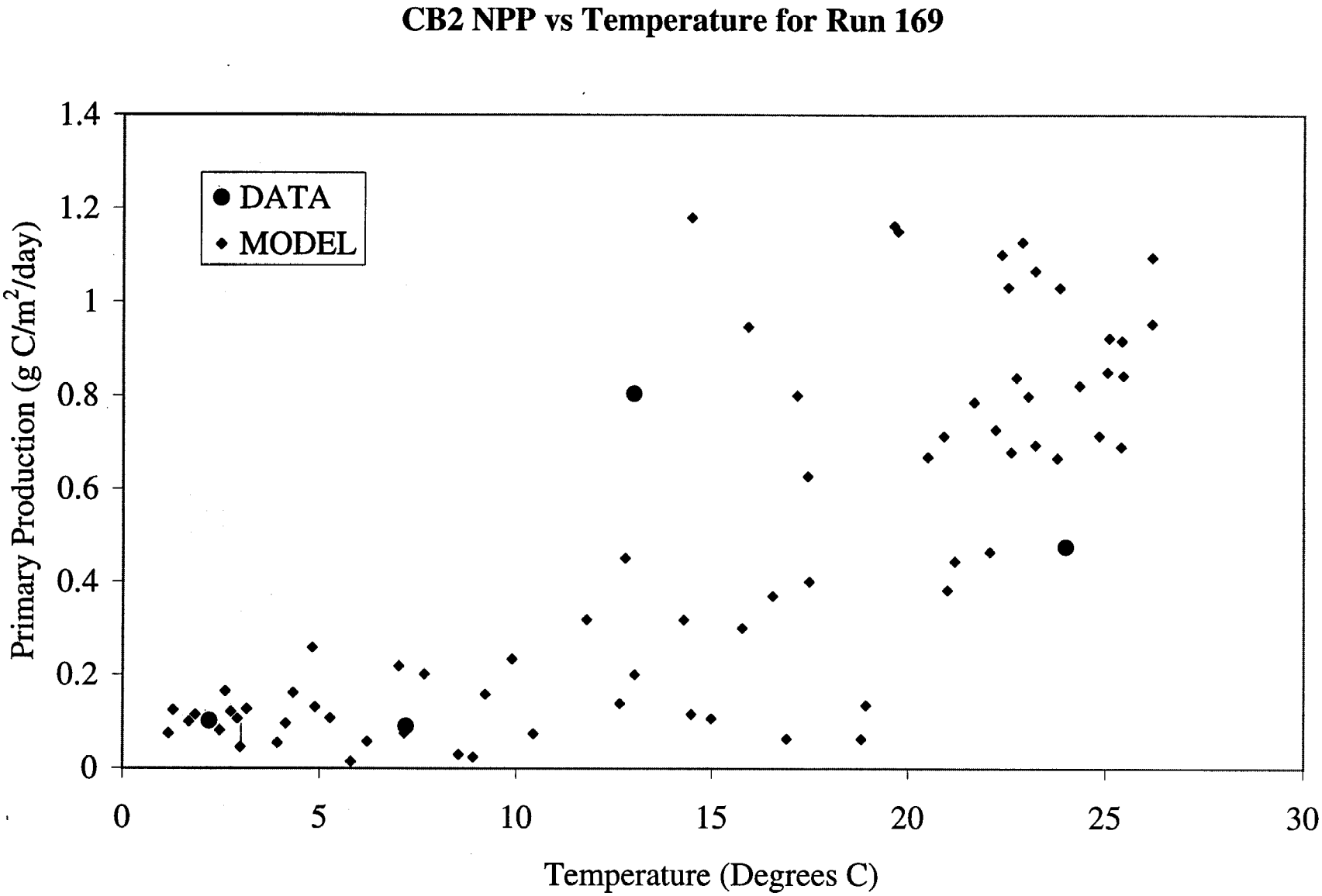
CB2 NPP vs Temperature for Run 169
DATA
MODEL
Primary Production (g C/m2/day)
1.4
1.2
1
0.8
0.6
0.4
0.2
0
0
5
10
15
20
25
30
Temperature (Degrees C)

Figure 50

CB3 and CB4 NPP vs Temperature for Run 169

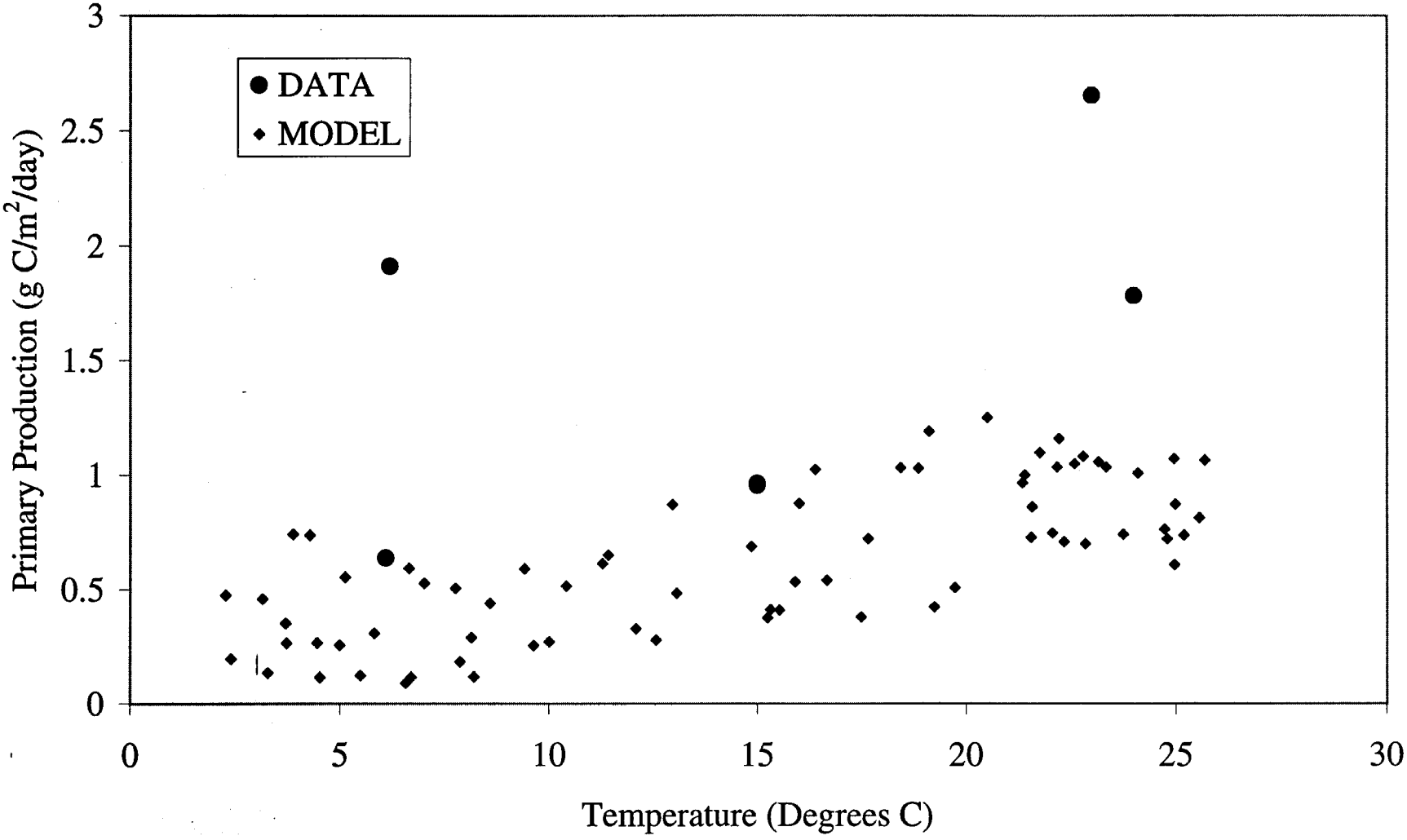

FIGURE 21

CB5 NPP vs Temperature for Run 169

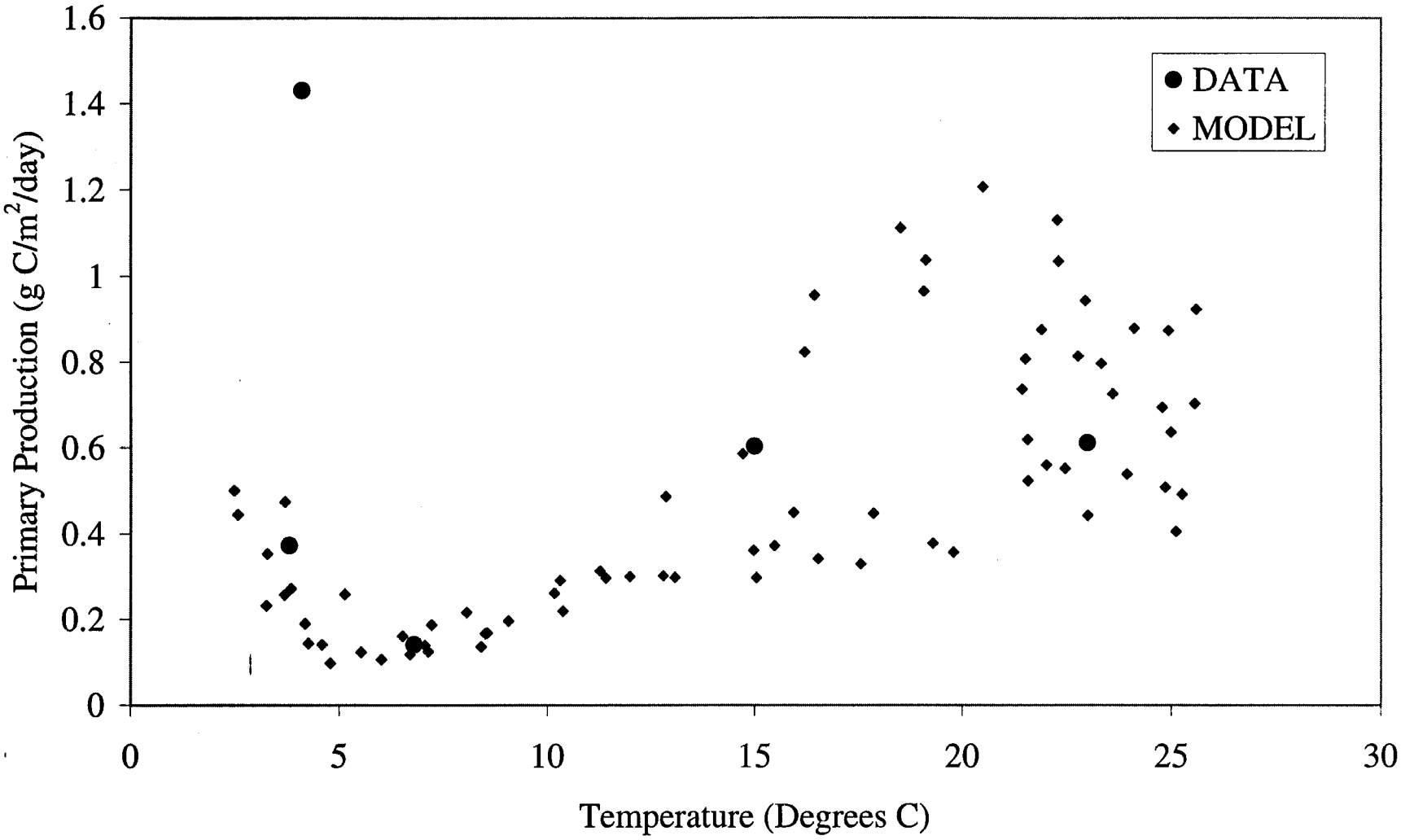

FIGURE 22

Malone NPP data vs Model Run 169 1985-1986 output

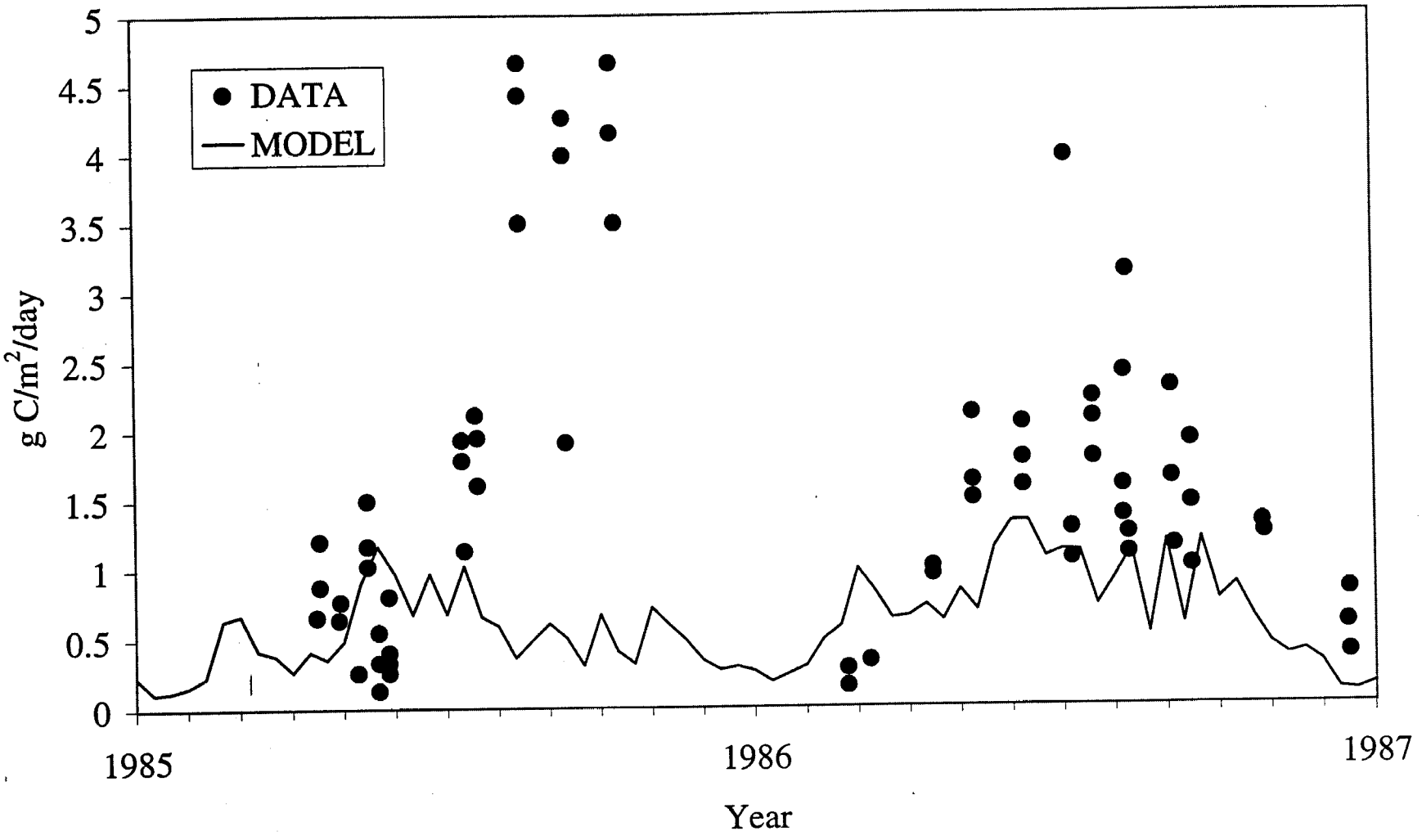

FIGURE 23

Upper Bay Primary Production

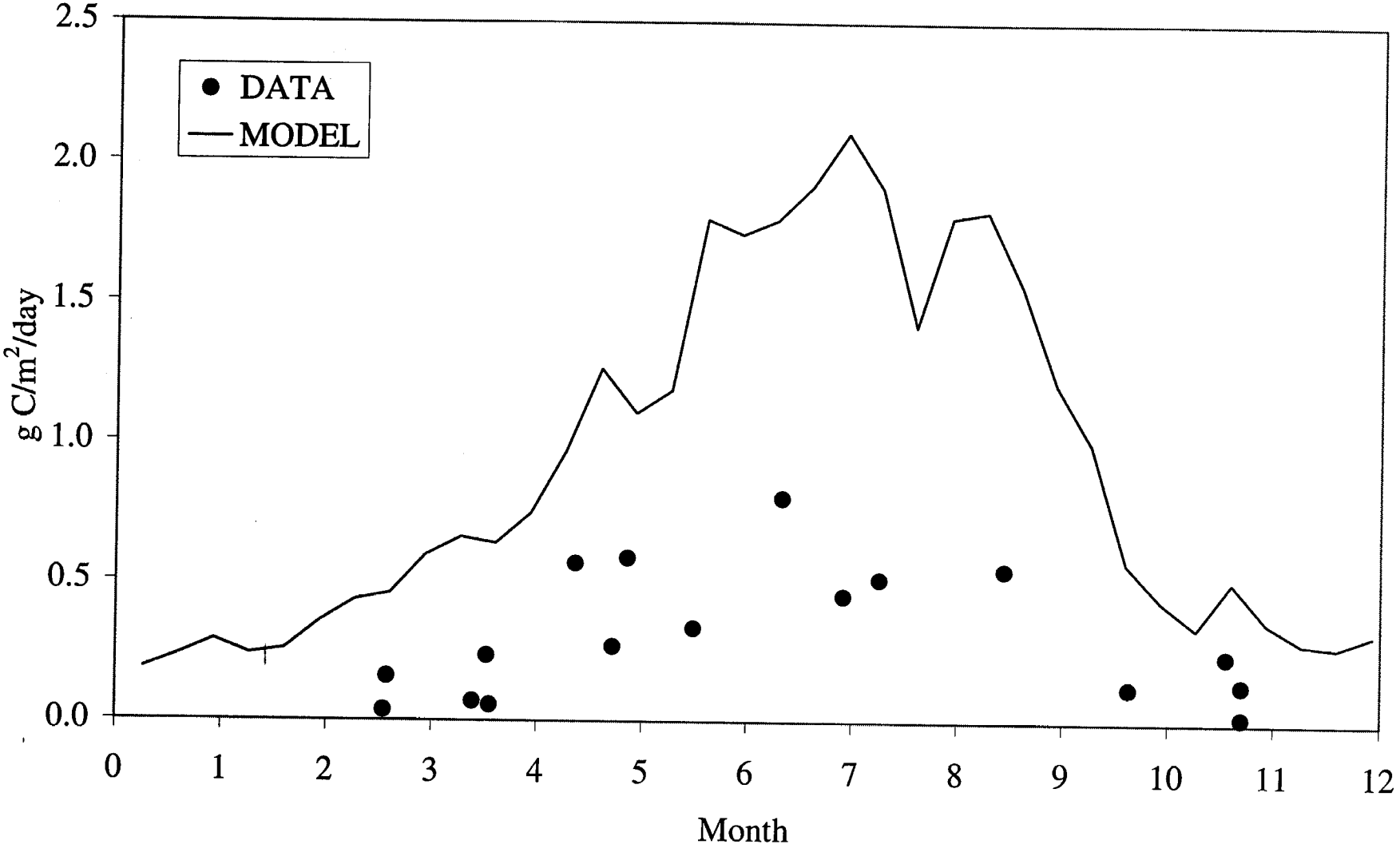

Figure 27

Middle Bay Primary Production

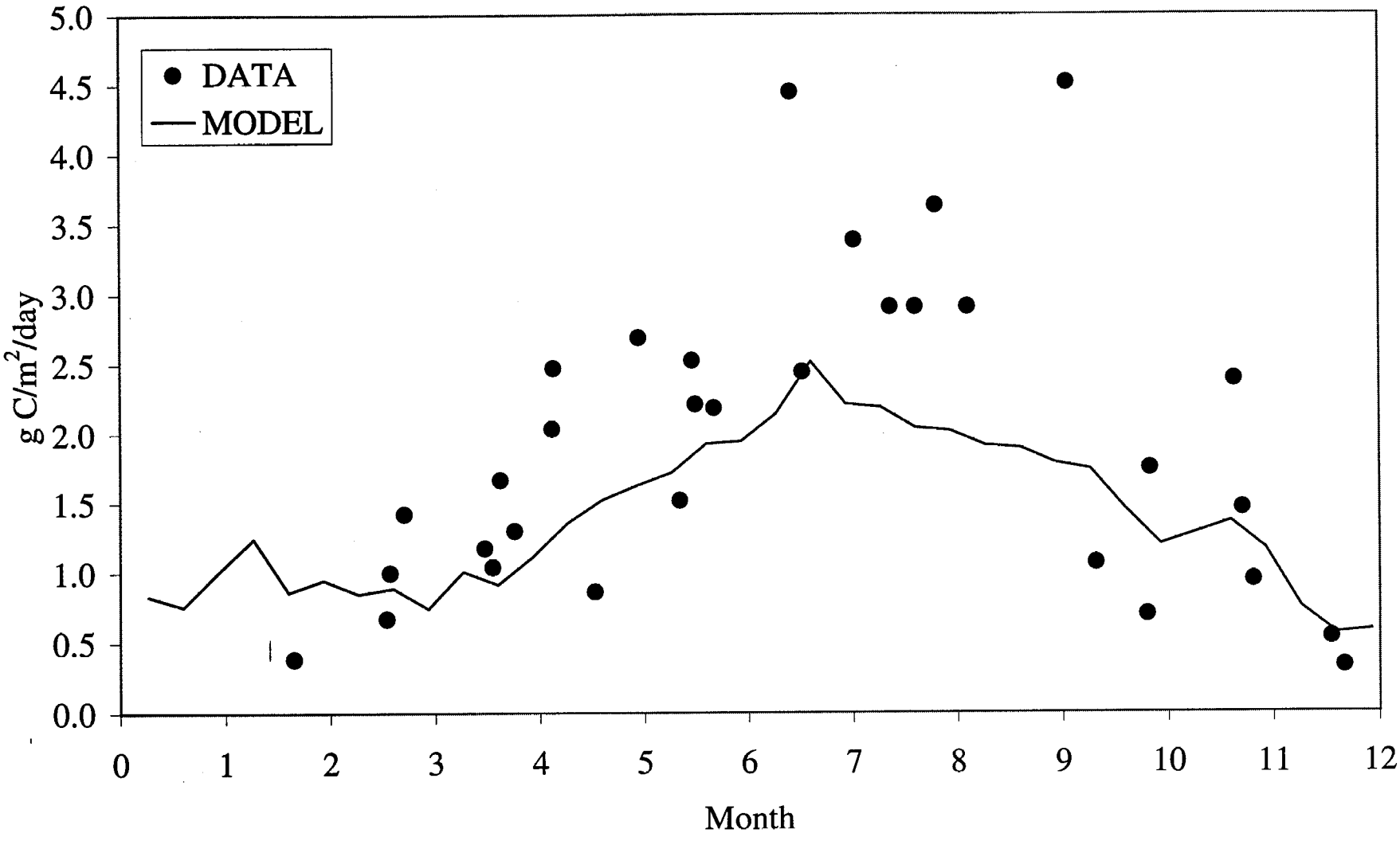

Figure 22

Lower Bay Primary Production

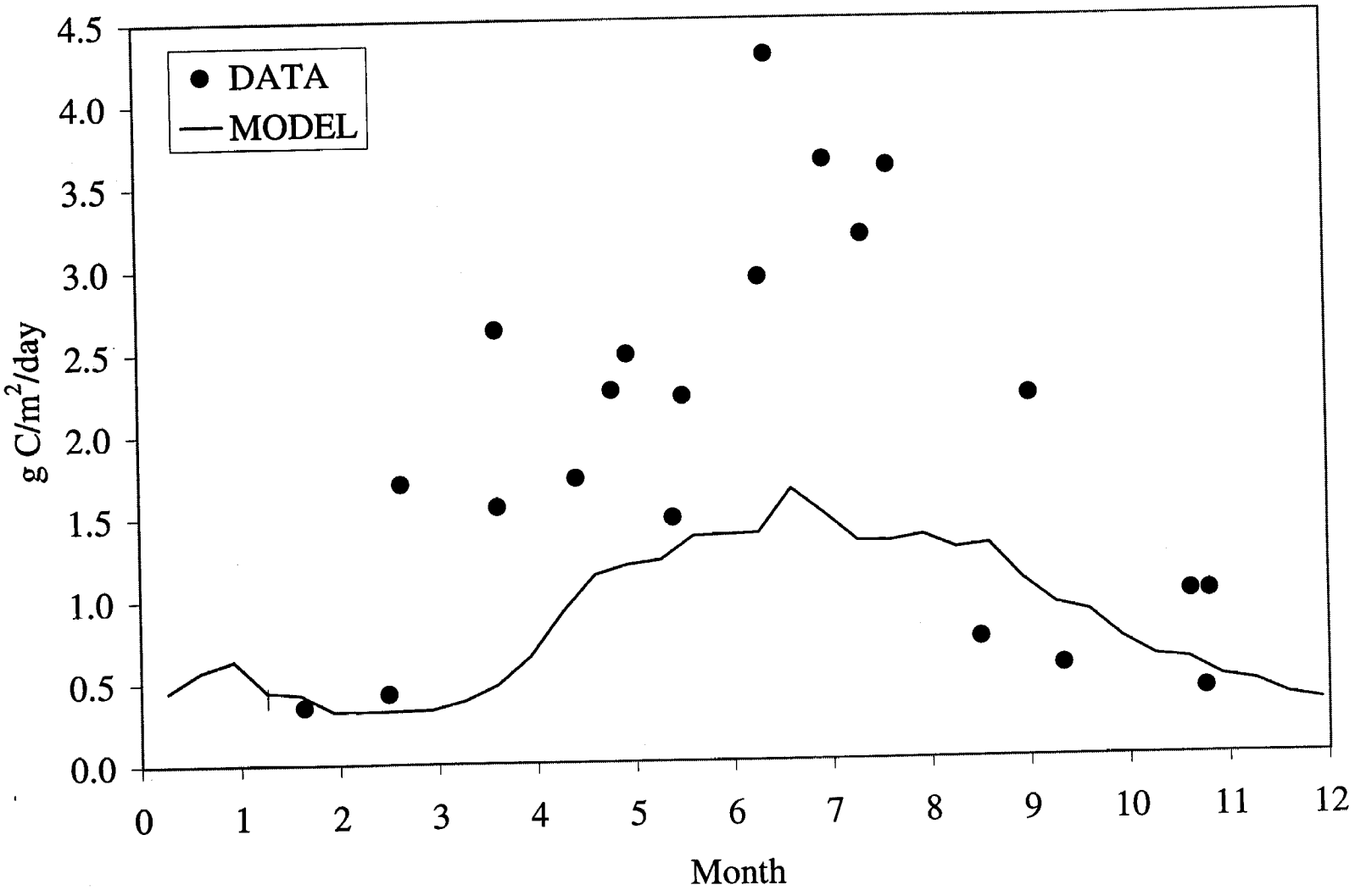

Figure 26

This report is to cited in the following way:
Cerco, C. 2000. Phytoplankton Kinetics in the Chesapeake Bay Estuary Model Technical Report. January, 2000. Chesapeake Bay Program Office, Annapolis, MD.
http://www.chesapeakebay.net/modsc.htm - Publications Tab. Date Retrieved: *retrieval date*